

# Per-link Parallel and Distributed Hybrid Beamforming for Multi-Cell Massive MIMO Millimeter Wave Full Duplex

Chandan Kumar Sheemar, and Dirk Slock

## Abstract

This article presents two novel hybrid beamforming (HYBF) designs for a multi-cell massive multiple-input-multiple-output (mMIMO) millimeter wave (mmWave) full duplex (FD) system under limited dynamic range (LDR). Firstly, we present a novel centralized (C-HYBF) scheme based on alternating optimization. However, C-HYBF presents many drawbacks such as high computational complexity, massive communication overhead to transfer complete channel state information (CSI) to the central node every channel coherence time (CCT), and requirement of expensive computational resources. To overcome these drawbacks, we present a very low complexity, per-link parallel and distributed HYBF (P&D-HYBF) scheme based on cooperation. Due to per-link decomposition, it enables each FD base station (BS) to solve its local sub-problems independently and in parallel on multiple processors, which leads to significant reduction in the execution time. It requires that each FD BS cooperates by exchanging information about the beamformers with the neighbouring BSs which allow each FD BS to adapt its beamformers correctly, and consequently, P&D-HYBF exhibits negligible performance loss compared to C-HYBF. Moreover, its complexity scales only linearly with the network size and density, making it highly scalable. Simulation results show that both designs achieve similar performance and outperform the fully digital half duplex (HD) system with only a few radio-frequency (RF) chains.

## I. INTRODUCTION

Cellular communication networks are continuously evolving to keep up with the escalating demands of the newly emerging wireless data services and maintain seamless connectivity. To accommodate the future data growth, the use of ultra-high-frequency bands such as the millimeter wave (mmWave) band has recently attracted considerable interest in the research community [1],

This work has been submitted to the IEEE for possible publication. Copyright may be transferred without notice, after which this version may no longer be accessible. An initial version of this work was part of the PhD thesis [1].

Chandan Kumar Sheemar is with the SnT department at the University of Luxembourg (email:chandankumar.sheemar@uni.lu). Dirk Slock is with the communication systems department at EURECOM, Sophia Antipolis, France (email:slock@eurecom.fr).

[2]. In contrast to the radio frequency (RF) and microwave bands, mmWave offers 200 greater spectrum, and due to its shorter wavelength, a massive number of antennas can be deployed in a tiny area [3]. Hybrid beamforming (HYBF) has been proposed as a prominent solution for mmWave to multiplex many data streams and achieve high beamforming gain with fewer RF chains, representing an optimal trade-off between performance and cost [4].

In parallel to the development of mmWave half duplex (HD) systems has been the progression of full duplex (FD) technology which enables the devices to simultaneously transmit and receive in the same frequency band which theoretically doubles the spectral efficiency [5]. Furthermore, FD can revolutionize a plethora of emerging technologies such as joint communication and sensing, low latency communications, can improve the security over wireless channels and provide more flexible utilization of the vast mmWave spectrum [6]–[8]. However, FD systems suffer from self-interference (SI), which can be 90 – 100 dB higher than the received signal power and advanced SI cancellation (SIC) techniques are hence required to cancel the SI to make FD operation viable.

#### *A. Prior Work and Motivation*

Recent studies on mmWave FD systems have shown that SIC is possible only with the aid of HYBF without additional hardware, thus making it very desirable. Achievable gains of HYBF in mmWave FD systems for a point-to-point and relays scenarios are investigated in [9]–[12] and [13]–[16], respectively. In [17], a novel HYBF design for a single-antenna multi-user mmWave FD system with 1-bit phase resolution is proposed. In [18], the performance of HYBF in mmWave FD aided with additional SIC hardware is investigated. In [19], achievable gain of mmWave FD system with one uplink (UL) and one downlink (DL) user only under the limited receive dynamic range is investigated. In [20], we presented a practical HYBF design for a single-cell massive MIMO (mMIMO) mmWave FD system under the limited dynamic range (LDR) noise model. In [21], the authors presented HYBF for a mmWave FD system including also sensing.

Although the papers above investigated HYBF for mmWave FD systems in many different scenario, we remark that the literature does not contribute to the multi-cell mMIMO mmWave FD systems with multi-antenna UL and DL users. Furthermore, no distributed beamforming design for the FD systems with UL and DL users, either for sub-6 GHz or mmWave, has ever been presented. To the best of our knowledge, the only existing solutions for distributed beamforming for FD are available for sub-6 GHz, limited only to FD relays [22]–[24] and point-to-point

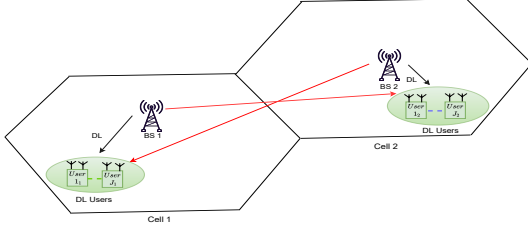


Fig. 1: Multi-cell HD system in DL.

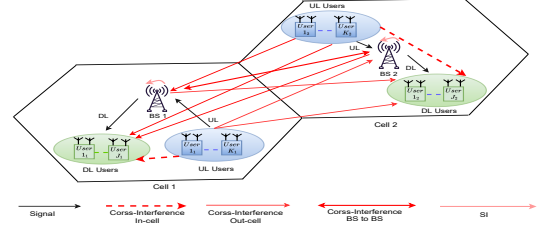


Fig. 2: Multi-cell FD system.

FD systems [25]. Finally, note also that no low-complexity HYBF design for the mmWave FD systems is yet available in the literature.

A multi-cell FD system represents a very challenging communication scenario as it suffers from many interference contributions, primarily engendered by cross-interference (CI) generated from the opposite transmission directions of the users, as shown in Figures 1-2. Hence, a vast amount of channel state information (CSI) is required to manage such interferences compared to the traditional HD systems. Centralized HYBF (C-HYBF) is undesirable for such a challenging scenario, and in general, as it would require complete CSI to be transferred to the central node every channel coherence time (CCT), e.g., based on a multi-hop communication, if the central node is located far from the network. Furthermore, the central node requires significant computational power to optimize many variables jointly for the UL and DL users. After the optimization, all the variables need to be communicated back to the FD BSs via feedback, and finally, each FD BS must communicate the optimized variables to its users. For any C-HYBF design, this procedure must be executed at the millisecond scale, which is prohibitive. Distributed HYBF, even though very challenging for FD systems, is a promising solution to cope with the aforementioned inherent challenges of centralized implementation and thus can reduce the communication overhead considerably. Per-link parallel and distributed (P&D)-HYBF can enable each BS to optimize beamformers for different users on multiple computational processors, thus leading to a very advanced distributed approach. For the literature on P&D beamforming for sub-6 GHz, we refer the reader to [26], [27].

## B. Main Contributions

We consider the problem of HYBF for weighted sum rate (WSR) maximization in a multi-cell mMIMO mmWave FD network with multi-antenna HD UL and DL users. The FD BSs and users are assumed to have hybrid and digital processing capabilities, respectively. Furthermore, they

are assumed to be equipped with non-ideal hardware, which is modelled by incorporating the LDR noise model [20], [28], leading to an impairment aware HYBF approach.

In general, centralized systems are superior to distributed systems and can serve as a benchmark to illustrate the performance loss due to distributed implementation. Therefore, we first present a novel C-HYBF scheme based on the minorization-maximization (MM) optimization technique by extending our work [20]. We then introduce P&D-HYBF for mmWave based on cooperation. Our design decomposes the multi-cell WSR maximization problem into per-link independent subproblems, which eliminates the problem of transferring full CSI to the central node every CCT. Due to the per-link decomposition, FD BSs can benefit from a multiprocessor capability and optimize many variables simultaneously. Being a cooperative design, P&D-HYBF requires information exchange about the beamformers and that each FD BS has access only to its local CSI. It is to be noted that per-link independent optimization for HYBF is non-trivial because the analog beamformers and analog combiners are common between the DL and UL users in the same cell, respectively. Moreover, the beamformers of the DL users are subject to a coupled total sum-power constraint imposed at the FD BSs, which is also affected by the analog beamformers. Our presented P&D-HYBF framework shows how to handle these coupling constraints in general and, therefore, can be adopted for future research on P&D-HYBF for both the FD and HD systems. Computational analysis shows that the complexity of C-HYBF and P&D-HYBF scales quadratically and only linearly as a function of both the network size and density, respectively, making the latter highly scalable and enabling the deployment of low-cost computational processors in each FD cell.

Simulation results show that P&D-HYBF scheme does not exhibit performance loss due to distributed implementation. Both designs achieve similar performance gains and outperform the conventional fully digital HD system with only a few RF chains and with very low phase-resolution at the analog stage of the FD BSs. The advantage of independent low-complexity computations for P&D-HYBF on different computational processors is investigated and results show that P&D-HYBF requires significantly less execution time compared to C-HYBF.

*Paper Organization:* The rest of the paper is organized as follows. First, we present the system model and problem formulation for the considered system in Section II. Then the MM optimization method and C-HYBF design is presented in Sections III and IV, respectively. Section V presents the P&D-HYBF design based on cooperation. Finally, Sections VI and VII present the simulation results and conclusions, respectively.

*Mathematical Notations:* Boldface lower and upper case characters denote vectors and matrices, respectively.  $\mathbb{E}\{\cdot\}$ ,  $\text{Tr}\{\cdot\}$ ,  $(\cdot)^H$ ,  $(\cdot)^T$ ,  $\otimes$ ,  $\mathbf{I}$ , and  $\mathbf{D}_d$  denote expectation, trace, conjugate transpose, transpose, kronecker product, identity matrix and the  $d$  dominant generalized eigenvectors selection matrix, respectively. Vector of zeros of size  $M$  is denoted as  $\mathbf{0}_{M \times 1}$ ,  $\text{vec}(\mathbf{X})$  stacks the column of  $\mathbf{X}$  into  $\mathbf{x}$ ,  $\text{unvec}(\mathbf{x})$  reshapes  $\mathbf{x}$  into  $\mathbf{X}$ , and  $\angle \mathbf{X}$  returns the phasors of matrix  $\mathbf{X}$ .  $\text{Cov}(\cdot)$  and  $\text{diag}(\cdot)$  denote the covariance and diagonal matrices, respectively, and  $\text{svd}(\mathbf{X})$  returns the singular value decomposition (SVD) of  $\mathbf{X}$ . Element of matrix  $\mathbf{X}$  at the  $m$ -th row and  $n$ -th column is denoted as  $\mathbf{X}(m, n)$ .

## II. SYSTEM MODEL

Let  $\mathcal{B} = \{1, \dots, B\}$  denote the set containing the indices of  $B$  FD BSs serving in  $B$  cells. Let  $\mathcal{D}_b = \{1, \dots, D_b\}$  and  $\mathcal{U}_b = \{1, \dots, U_b\}$  denote the sets containing the indices of  $D_b$  DL and  $U_b$  UL multi-antenna HD users communicating with BS  $b \in \mathcal{B}$ . The DL user  $j_b \in \mathcal{D}_b$  and UL user  $k_b \in \mathcal{U}_b$  are assumed to have  $N_{j_b}$  receive and  $M_{k_b}$  transmit antennas, respectively. The FD BS  $b \in \mathcal{B}$  is assumed to have  $M_b^{RF}$  and  $N_b^{RF}$  transmit and receive RF chains, respectively, and  $M_b$  and  $N_b$  transmit and receive antennas, respectively. We denote with  $\mathbf{V}_{j_b} \in \mathbb{C}^{M_b^{RF} \times d_{j_b}}$  and  $\mathbf{U}_{k_b} \in \mathbb{C}^{M_{k_b} \times d_{k_b}}$  the digital beamformers for the white unitary variance data streams  $\mathbf{s}_{j_b} \in \mathbb{C}^{d_{j_b} \times 1}$  and  $\mathbf{s}_{k_b} \in \mathbb{C}^{d_{k_b} \times 1}$  transmitted for DL user  $j_b \in \mathcal{D}_b$  and from UL user  $k_b \in \mathcal{U}_b$ , respectively. Let  $\mathbf{G}_b^{RF} \in \mathbb{C}^{M_b \times M_b^{RF}}$  and  $\mathbf{F}_b^{RF} \in \mathbb{C}^{N_b^{RF} \times N_b}$  denote the fully connected analog beamformer and analog combiner for FD BS  $b \in \mathcal{B}$ , respectively. Let  $\mathcal{P}_b = \{1, e^{i2\pi/n_b}, e^{i4\pi/n_b}, \dots, e^{i2\pi n_b - 1/n_b}\}$  denote the set of  $n_b$  possible discrete values that the unit-modulus elements of  $\mathbf{G}_b^{RF}$  and  $\mathbf{F}_b^{RF}$  can assume. Let  $\mathbb{Q}_b(\cdot)$  denote the quantizer function to quantize the infinite resolution unit-modulus elements of  $\mathbf{G}_b^{RF}$  ( $\mathbf{F}_b^{RF}$ ) such that  $\mathbb{Q}_b(\angle \mathbf{G}_b^{RF}(m, n))(\mathbb{Q}_b(\angle \mathbf{F}_b^{RF}(m, n))) \in \mathcal{P}_b, \forall m, n$ .

The users and the FD BSs are assumed to be suffering from the LDR noise due to non-ideal hardware. It is denoted as  $\mathbf{c}_{k_b}$  and  $\mathbf{e}_{j_b}$  for the UL user  $k_b \in \mathcal{U}_b$  and DL user  $j_b \in \mathcal{D}_b$ , respectively, modelled as [28]

$$\mathbf{c}_{k_b} \sim \mathcal{CN}(\mathbf{0}_{M_{k_b} \times 1}, k_{k_b} \text{diag}(\mathbf{U}_{k_b} \mathbf{U}_{k_b}^H)), \quad \mathbf{e}_{j_b} \sim \mathcal{CN}(\mathbf{0}_{N_{j_b} \times 1}, \beta_{j_b} \text{diag}(\mathbf{\Phi}_{j_b})), \quad (1)$$

where  $k_{k_b} \ll 1$ ,  $\beta_{j_b} \ll 1$ ,  $\mathbf{\Phi}_{j_b} = \text{Cov}(\mathbf{r}_{j_b})$  and  $\mathbf{r}_{j_b}$  denotes the undistorted received signal for DL user  $j_b \in \mathcal{D}_b$ . Let  $\mathbf{c}_b$  and  $\mathbf{e}_b$  denote the transmit and receive LDR noise for a hybrid FD BS  $b \in \mathcal{B}$ , respectively, which can be modelled as [20]

$$\mathbf{c}_b \sim \mathcal{CN}(\mathbf{0}_{M_b \times 1}, k_b \text{diag}(\sum_{n_b \in \mathcal{D}_b} \mathbf{G}_b \mathbf{V}_{n_b} \mathbf{V}_{n_b}^H \mathbf{G}_b^H)), \quad \mathbf{e}_b \sim \mathcal{CN}(\mathbf{0}_{N_b^{RF} \times 1}, \beta_b \text{diag}(\mathbf{\Phi}_b)), \quad (2)$$

with  $k_b \ll 1$ ,  $\beta_b \ll 1$ ,  $\mathbf{\Phi}_b = \text{Cov}(\mathbf{r}_b)$  and  $\mathbf{r}_b$  denotes the undistorted received signal by FD BS  $b \in \mathcal{B}$  after the analog combiner  $\mathbf{F}_b^{RF}$ . The thermal noise for FD BS  $b \in \mathcal{B}$  and DL user  $j_b \in \mathcal{D}_b$  is denoted as  $\mathbf{n}_b$  and  $\mathbf{n}_{j_b}$ , with variances  $\sigma_b^2$  and  $\sigma_{j_b}^2$ , respectively, and modelled as

$$\mathbf{n}_b \sim \mathcal{CN}(\mathbf{0}_{N_b \times 1}, \sigma_b^2 \mathbf{I}), \quad \mathbf{n}_{j_b} \sim \mathcal{CN}(\mathbf{0}_{N_{j_b} \times 1}, \sigma_{j_b}^2 \mathbf{I}). \quad (3)$$

### A. Channel Modelling

We assume perfect CSI and let  $\mathbf{H}_{j_b} \in \mathbb{C}^{N_{j_b} \times M_b}$  and  $\mathbf{H}_{k_b} \in \mathbb{C}^{N_b \times M_{k_b}}$  denote the direct channels responses between the DL user  $j_b \in \mathcal{D}_b$  and UL user  $k_b \in \mathcal{U}_b$ , respectively, and their serving FD BS  $b \in \mathcal{B}$ . Let  $\mathbf{H}_{j_b, k_b} \in \mathbb{C}^{N_{j_b} \times M_{k_b}}$  and  $\mathbf{H}_{j_b, k_c} \in \mathbb{C}^{N_{j_b} \times M_{k_c}}$  denote the in-cell UL CI channel response between the DL user  $j_b \in \mathcal{D}_b$  and UL user  $k_b \in \mathcal{U}_b$  and the out-cell UL CI channel response between the DL user  $j_b \in \mathcal{D}_b$  and UL user  $k_c \in \mathcal{U}_c$ , respectively, with  $b \neq c$ . Let  $\mathbf{H}_{j_b, c} \in \mathbb{C}^{N_{j_b} \times M_c}$  and  $\mathbf{H}_{b, k_c} \in \mathbb{C}^{N_b \times M_{k_c}}$  denote the interference channels responses from FD BS  $c \in \mathcal{B}$  to DL user  $j_b \in \mathcal{D}_b$  and from UL user  $k_c \in \mathcal{U}_c$  to FD BS  $b$ , respectively, with  $c \neq b$ . Let  $\mathbf{H}_{b, c} \in \mathbb{C}^{N_b \times M_c}$  and  $\mathbf{H}_{b, b} \in \mathbb{C}^{N_b \times M_b}$  denote the DL CI channel response from FD BS  $c \in \mathcal{B}$  to FD BS  $b \in \mathcal{B}$ , with  $c \neq b$ , and the SI channel response for FD BS  $b \in \mathcal{B}$ , respectively.

In mmWave, channel response  $\mathbf{H}_{k_b}$  can be modelled as [29]

$$\mathbf{H}_{k_b} = \sqrt{\frac{1}{N_{k_b}}} \sum_{n=1}^{N_{k_b}^p} \alpha_{k_b}^n \mathbf{a}_r^b(\phi_{k_b}^n) \mathbf{a}_t^{k_b}(\theta_{k_b}^n)^T. \quad (4)$$

The scalars  $N_{k_b}^p$  and  $\alpha_{k_b}^n$  denote the number of paths and a complex Gaussian random variable with amplitudes and phases distributed according to the Rayleigh and uniform distribution, respectively. The vectors  $\mathbf{a}_r^b(\phi_{k_b}^n)$  and  $\mathbf{a}_t^{k_b}(\theta_{k_b}^n)^T$  denote the receive and transmit antenna array response for FD BS  $b \in \mathcal{B}$  and UL user  $k_b \in \mathcal{U}_b$ , respectively, with the angle of arrival (AoA)  $\phi_{k_b}^n$  and angle of departure (AoD)  $\theta_{k_b}^n$ , respectively. The channel responses  $\mathbf{H}_{j_b}$ ,  $\mathbf{H}_{j_b, k_b}$ ,  $\mathbf{H}_{j_b, k_c}$ ,  $\mathbf{H}_{j_b, c}$  and  $\mathbf{H}_{b, k_c}$  can be modelled similarly as (4) and the SI channel  $\mathbf{H}_{b, b} \in \mathbb{C}^{N_b \times M_b}$  can be modelled as [20]

$$\mathbf{H}_b = \sqrt{\frac{\kappa_b}{\kappa_b + 1}} \mathbf{H}_b^L + \sqrt{\frac{1}{\kappa_b + 1}} \mathbf{H}_b^R, \quad \text{where} \quad \mathbf{H}_b^L(m, n) = \frac{\rho_b}{r_{m,n}} e^{-j2\pi \frac{r_{m,n}}{\lambda}}. \quad (5)$$

The matrices  $\mathbf{H}_b^L$  and  $\mathbf{H}_b^R$  denote the line-of-sight (LoS) and reflected components channel response of the SI channel, respectively. The scalars  $\kappa_b$ ,  $\rho_b$ ,  $r_{m,n}$  and  $\lambda$  denote the Rician factor, the power normalization constant to assure  $\mathbb{E}(\|\mathbf{H}_b^L(m, n)\|_F^2) = M_b N_b$  [9], the distance between  $m$ -th receive and  $n$ -th transmit antenna and the wavelength, respectively. Note that also the channel matrix  $\mathbf{H}_b^R$  for the reflected components can also be modelled as (4).

## B. Problem Formulation

Let  $\mathbf{y}_{j_b}$  and  $\mathbf{y}_{k_b}$  denote the signals received by the DL user  $j_b \in \mathcal{D}_b$  and by the FD BS  $b \in \mathcal{B}$  from UL user  $k_b \in \mathcal{U}_b$  after the analog combiner  $\mathbf{F}_b^{RF}$ , respectively, which can be written as

$$\begin{aligned} \mathbf{y}_{j_b} = & \mathbf{H}_{j_b} \left( \sum_{n_b \in \mathcal{D}_b} \mathbf{G}_b^{RF} \mathbf{V}_{n_b} \mathbf{s}_{n_b} + \mathbf{c}_b \right) + \mathbf{e}_{j_b} + \mathbf{n}_{j_b} + \sum_{k_b \in \mathcal{U}_b} \mathbf{H}_{j_b, k_b} (\mathbf{U}_{k_b} \mathbf{s}_{k_b} + \mathbf{c}_{k_b}) \\ & + \sum_{c \in \mathcal{B}, c \neq b} \mathbf{H}_{j_b, c} \left( \sum_{n_c \in \mathcal{D}_c} \mathbf{G}_c^{RF} \mathbf{V}_{n_c} \mathbf{s}_{n_c} + \mathbf{c}_c \right) + \sum_{c \in \mathcal{B}, c \neq b} \sum_{k_c \in \mathcal{U}_c} \mathbf{H}_{j_b, k_c} (\mathbf{U}_{k_c} \mathbf{s}_{k_c} + \mathbf{c}_{k_c}), \end{aligned} \quad (6)$$

$$\begin{aligned} \mathbf{y}_{k_b} = & \mathbf{F}_b^{RFH} \left( \sum_{k_b \in \mathcal{U}_b} \mathbf{H}_{k_b} (\mathbf{U}_{k_b} \mathbf{s}_{k_b} + \mathbf{c}_{k_b}) + \mathbf{n}_b + \mathbf{H}_{b, b} \left( \sum_{j_b \in \mathcal{D}_b} \mathbf{G}_b^{RF} \mathbf{V}_{j_b} \mathbf{s}_{j_b} + \mathbf{c}_b \right) \right. \\ & \left. + \sum_{c \in \mathcal{B}, c \neq b} \mathbf{H}_{b, c} \left( \sum_{j_c \in \mathcal{D}_c} \mathbf{G}_c^{RF} \mathbf{V}_{j_c} \mathbf{s}_{j_c} + \mathbf{c}_c \right) + \sum_{c \in \mathcal{B}, c \neq b} \sum_{k_c \in \mathcal{U}_c} \mathbf{H}_{b, k_c} (\mathbf{U}_{k_c} \mathbf{s}_{k_c} + \mathbf{c}_{k_c}) \right) + \mathbf{e}_b. \end{aligned} \quad (7)$$

Let  $\bar{k}_b$ ,  $\bar{j}_b$  and  $\bar{b}$  denote the indices in the sets  $\mathcal{U}_b$ ,  $\mathcal{D}_b$  and  $\mathcal{B}$  without the elements  $k_b$ ,  $j_b$  and  $b$ , respectively. Let  $\mathbf{T}_{k_b} \triangleq \mathbf{U}_{k_b} \mathbf{U}_{k_b}^H$  and  $\mathbf{Q}_{j_b} \triangleq \mathbf{G}_b \mathbf{V}_{j_b} \mathbf{V}_{j_b}^H \mathbf{G}_b^H$  denote the transmit covariance matrices of UL user  $k_b \in \mathcal{U}_b$  and of FD BS  $b \in \mathcal{B}$  intended for its DL user  $j_b \in \mathcal{D}_b$ , respectively. Let  $(\mathbf{R}_{k_b})$   $\mathbf{R}_{\bar{k}_b}$  and  $(\mathbf{R}_{j_b})$   $\mathbf{R}_{\bar{j}_b}$  denote the (signal plus) interference plus noise covariance matrices received by the FD BS  $b \in \mathcal{B}$  from UL user  $k_b \in \mathcal{U}_b$  and by the DL user  $j_b \in \mathcal{D}_b$ , respectively.

The matrices  $\mathbf{R}_{k_b}$  and  $\mathbf{R}_{j_b}$  can be written as follows

$$\begin{aligned} \mathbf{R}_{j_b} = & \mathbf{H}_{j_b} \mathbf{Q}_{j_b} \mathbf{H}_{j_b}^H + \mathbf{H}_{j_b} \left( \sum_{\substack{n_b \in \mathcal{D}_b \\ n_b \neq j_b}} \mathbf{Q}_{n_b} \right) \mathbf{H}_{j_b}^H + \mathbf{H}_{j_b} k_b \text{diag} \left( \sum_{n_b \in \mathcal{D}_b} \mathbf{Q}_{n_b} \right) \mathbf{H}_{j_b}^H \\ & + \sum_{k_b \in \mathcal{U}_b} \mathbf{H}_{j_b, k_b} (\mathbf{T}_{k_b} + k_{k_b} \text{diag}(\mathbf{T}_{k_b})) \mathbf{H}_{j_b, k_b}^H + \sum_{\substack{c \in \mathcal{B} \\ c \neq b}} \mathbf{H}_{j_b, c} \left( \sum_{n_c \in \mathcal{D}_c} \mathbf{Q}_{n_c} + k_c \text{diag}(\mathbf{Q}_{n_c}) \right) \mathbf{H}_{j_b, c}^H \quad (8a) \\ & + \sum_{\substack{c \in \mathcal{B} \\ c \neq b}} \sum_{k_c \in \mathcal{U}_c} \mathbf{H}_{j_b, k_c} (\mathbf{T}_{k_c} + k_{k_c} \text{diag}(\mathbf{T}_{k_c})) \mathbf{H}_{j_b, k_c}^H + \beta_{j_b} \text{diag}(\Phi_{j_b}) + \sigma_{j_b}^2 \mathbf{I}_{N_{j_b}}, \end{aligned}$$

$$\begin{aligned} \mathbf{R}_{k_b} = & \mathbf{F}_b^{RFH} \left( \mathbf{H}_{k_b} \mathbf{T}_{k_b} \mathbf{H}_{k_b}^H + \sum_{\substack{m_b \in \mathcal{U}_b \\ m_b \neq k_b}} \mathbf{H}_{m_b} \mathbf{T}_{m_b} \mathbf{H}_{m_b}^H + \sum_{m_b \in \mathcal{U}_b} k_{m_b} \mathbf{H}_{m_b} \text{diag}(\mathbf{T}_{m_b}) \mathbf{H}_{m_b}^H \right. \\ & \left. + \mathbf{H}_{b, b} \sum_{j_b \in \mathcal{D}_b} (\mathbf{Q}_{j_b} + k_b \text{diag}(\mathbf{Q}_{j_b})) \mathbf{H}_{b, b}^H + \sum_{\substack{c \in \mathcal{B} \\ c \neq b}} \mathbf{H}_{b, c} \sum_{j_c \in \mathcal{D}_c} (\mathbf{Q}_{j_c} + k_c \text{diag}(\mathbf{Q}_{j_c})) \mathbf{H}_{b, c}^H \right. \quad (8b) \\ & \left. + \sum_{\substack{c \in \mathcal{B} \\ c \neq b}} \sum_{k_c \in \mathcal{U}_c} \mathbf{H}_{b, k_c} (\mathbf{T}_{k_c} + k_{k_c} \text{diag}(\mathbf{T}_{k_c})) \mathbf{H}_{b, k_c}^H + \sigma_b^2 \mathbf{I}_{N_b} \right) \mathbf{F}_b^{RF} + \beta_b \text{diag}(\Phi_b), \end{aligned}$$

and  $\mathbf{R}_{\bar{k}_b}$  and  $\mathbf{R}_{\bar{j}_b}$  can be obtained as  $\mathbf{R}_{\bar{k}_b} = \mathbf{R}_{k_b} - \mathbf{H}_{j_b} \mathbf{Q}_{j_b} \mathbf{H}_{j_b}^H$  and  $\mathbf{R}_{\bar{j}_b} = \mathbf{R}_{j_b} - \mathbf{F}_b^{RFH} \mathbf{H}_{k_b} \mathbf{T}_{k_b} \mathbf{H}_{k_b}^H \mathbf{F}_b^{RF}$ , respectively.

The WSR maximization problem for HYBF in a multi-cell mMIMO mmWave FD system with  $J_b$  DL and  $U_b$  UL multi-antenna users  $\forall b \in \mathcal{B}$ , under the joint sum-power, unit-modulus and discrete phase-shifters constraints can be stated as

$$\max_{\mathbf{U}, \mathbf{V}, \mathbf{G}^{RF}, \mathbf{F}^{RF}} \sum_{b \in \mathcal{B}} \sum_{k_b \in \mathcal{U}_b} w_{k_b} \text{Indet}(\mathbf{R}_{k_b}^{-1} \mathbf{R}_{k_b}) + \sum_{b \in \mathcal{B}} \sum_{j_b \in \mathcal{D}_b} w_{j_b} \text{Indet}(\mathbf{R}_{j_b}^{-1} \mathbf{R}_{j_b}) \quad (9a)$$

$$\text{s.t.} \quad \text{Tr}(\mathbf{U}_{k_b} \mathbf{U}_{k_b}^H) \leq p_{k_b}, \quad \forall k_b \in \mathcal{U}_b, \quad (9b)$$

$$\text{Tr}\left(\sum_{j \in \mathcal{D}_b} \mathbf{G}_b \mathbf{V}_j \mathbf{V}_j^H \mathbf{G}_b^H\right) \leq p_b, \quad \forall b \in \mathcal{B}, \quad (9c)$$

$$\mathbf{G}_b^{RF}(m, n) \text{ and } \mathbf{F}_b^{RF}(m, n) \in \mathcal{P}_b, \quad \forall m, n \text{ \& } \forall b \in \mathcal{B}. \quad (9d)$$

The scalars  $w_{k_b}$  and  $w_{j_b}$  denote rate weights for UL user  $k_b \in \mathcal{U}_b$  and DL user  $j_b \in \mathcal{D}_b$ , respectively, and the scalars  $p_{k_b}$  and  $p_b$  denote the sum-power constraint for UL user  $k_b \in \mathcal{U}_b$  and FD BS  $b \in \mathcal{B}$ , respectively. The collections of digital beamformers in UL and DL are denoted as  $\mathbf{U}$  and  $\mathbf{V}$ , respectively, and the collections of analog beamformers and combiners are denoted as  $\mathbf{G}^{RF}$  and  $\mathbf{F}^{RF}$ , respectively.

### III. MINORIZATION-MAXIMIZATION

Problem (9) is non-concave in the transmit covariance matrices  $\mathbf{T}_{k_b}$  and  $\mathbf{Q}_{j_b}$  due to the interference terms and finding its global optimum is very challenging. To find its sub-optimal solution based on alternating optimization, we leverage the minorization-maximization (MM) method [30], which allows to reformulate (9) with its minorizer using the difference-of-convex (DC) programming [30].

Let  $\text{WR}_{k_b}^{UL}$  and  $\text{WR}_{j_b}^{DL}$  denote the weighted rate (WR) of users  $k_b \in \mathcal{U}_b$  and  $j_b \in \mathcal{D}_b$ , respectively, and let  $\text{WSR}_{k_b}^{UL}$  and  $\text{WSR}_{j_b}^{DL}$  denote the WSR of users outside the cell  $b$  in UL and DL, respectively. The dependence of the global WSR in (9) on the aforementioned terms can be highlighted as

$$\text{WSR} = \text{WR}_{k_b}^{UL} + \text{WSR}_{k_b}^{UL} + \text{WR}_{j_b}^{DL} + \text{WSR}_{j_b}^{DL} + \text{WSR}_b^{UL} + \text{WSR}_b^{DL}. \quad (10)$$

Note that in (10), the WSR in UL and DL for FD BS  $b \in \mathcal{B}$  is given as  $\text{WSR}_b^{UL} = \text{WR}_{k_b}^{UL} + \text{WSR}_{k_b}^{UL}$  and  $\text{WSR}_b^{DL} = \text{WR}_{j_b}^{DL} + \text{WSR}_{j_b}^{DL}$ , respectively. Considering the dependence of the transmit covariance matrices on the global WSR, only  $\text{WR}_{k_b}^{UL}$  is concave in  $\mathbf{T}_{k_b}$  and  $\text{WSR}_{k_b}^{UL}$ ,  $\text{WSR}_b^{DL}$ ,  $\text{WSR}_b^{UL}$  and  $\text{WSR}_{j_b}^{DL}$  are non concave in  $\mathbf{T}_{k_b}$  due to interference. Similarly, only  $\text{WR}_{j_b}^{DL}$  is



TABLE I: Gradients expressions to construct the minorized WSR cost function.

$\hat{\mathbf{G}}_{k_b,b}^{UL}$	$\sum_{\substack{m_b \in \mathcal{U}_b \\ m_b \neq k_b}} w_{m_b} [\mathbf{H}_{m_b}^H \mathbf{F}_b^{RF} (\mathbf{R}_{m_b}^{-1} - \mathbf{R}_{m_b}^{-1} + \beta_b \text{diag}(\mathbf{R}_{m_b}^{-1} - \mathbf{R}_{m_b}^{-1})) \mathbf{F}_b^{RFH} \mathbf{H}_{m_b} + k_{m_b} \text{diag}(\mathbf{H}_{m_b}^H \mathbf{F}_b^{RF} (\mathbf{R}_{m_b}^{-1} - \mathbf{R}_{m_b}^{-1}) \mathbf{F}_b^{RFH} \mathbf{H}_{m_b})].$
$\hat{\mathbf{G}}_{k_b,b}^{DL}$	$\sum_{j_b \in \mathcal{D}_b} w_{j_b} [\mathbf{H}_{j_b,k_b}^H (\mathbf{R}_{j_b}^{-1} - \mathbf{R}_{j_b}^{-1} + \beta_{j_b} \text{diag}(\mathbf{R}_{j_b}^{-1} - \mathbf{R}_{j_b}^{-1})) \mathbf{H}_{j_b,k_c} + k_{k_b} \text{diag}(\mathbf{H}_{j_b,k_b}^H (\mathbf{R}_{j_b}^{-1} - \mathbf{R}_{j_b}^{-1}) \mathbf{H}_{j_b,k_b})]$
$\hat{\mathbf{G}}_{k_b,\bar{b}}^{UL}$	$\sum_{\substack{c \in \mathcal{B} \\ c \neq b}} \sum_{k_c \in \mathcal{U}_c} w_{k_c} [\mathbf{H}_{c,k_b}^H \mathbf{F}_c^{RF} (\mathbf{R}_{k_c}^{-1} - \mathbf{R}_{k_c}^{-1} + \beta_c \text{diag}(\mathbf{R}_{k_c}^{-1} - \mathbf{R}_{k_c}^{-1})) \mathbf{F}_c^{RFH} \mathbf{H}_{c,k_b} + k_{k_b} \text{diag}(\mathbf{H}_{c,k_b}^H \mathbf{F}_c^{RF} (\mathbf{R}_{k_c}^{-1} - \mathbf{R}_{k_c}^{-1}) \mathbf{F}_c^{RFH} \mathbf{H}_{c,k_b})]$
$\hat{\mathbf{G}}_{k_b,\bar{b}}^{DL}$	$\sum_{\substack{c \in \mathcal{B} \\ c \neq b}} \sum_{j_c \in \mathcal{D}_c} w_{j_c} [\mathbf{H}_{j_c,k_b}^H (\mathbf{R}_{j_c}^{-1} - \mathbf{R}_{j_c}^{-1} + \beta_{j_c} \text{diag}(\mathbf{R}_{j_c}^{-1} - \mathbf{R}_{j_c}^{-1})) \mathbf{H}_{c,k_b} + k_{k_b} \text{diag}(\mathbf{H}_{c,k_b}^H (\mathbf{R}_{j_c}^{-1} - \mathbf{R}_{j_c}^{-1}) \mathbf{H}_{c,k_b})]$
$\hat{\mathbf{G}}_{j_b,b}^{UL}$	$\sum_{k_b \in \mathcal{U}_b} w_{k_b} [\mathbf{H}_{b,b}^H \mathbf{F}_b^{RF} (\mathbf{R}_{k_b}^{-1} - \mathbf{R}_{k_b}^{-1} + \beta_b \text{diag}(\mathbf{R}_{k_b}^{-1} - \mathbf{R}_{k_b}^{-1})) \mathbf{F}_b^{RFH} \mathbf{H}_{b,b} + k_{k_b} \text{diag}(\mathbf{H}_{b,b}^H \mathbf{F}_b^{RF} (\mathbf{R}_{k_b}^{-1} - \mathbf{R}_{k_b}^{-1}) \mathbf{F}_b^{RFH} \mathbf{H}_{b,b})]$
$\hat{\mathbf{G}}_{j_b,b}^{DL}$	$\sum_{\substack{l_b \in \mathcal{D}_b \\ l_b \neq j_b}} w_{l_b} [\mathbf{H}_{l_b}^H (\mathbf{R}_{l_b}^{-1} - \mathbf{R}_{l_b}^{-1} + \beta_{l_b} \text{diag}(\mathbf{R}_{l_b}^{-1} - \mathbf{R}_{l_b}^{-1})) \mathbf{H}_{l_b}^H + k_c \text{diag}(\mathbf{H}_{l_b}^H (\mathbf{R}_{l_b}^{-1} - \mathbf{R}_{l_b}^{-1}) \mathbf{H}_{l_b})]$
$\hat{\mathbf{G}}_{j_b,\bar{b}}^{UL}$	$\sum_{\substack{c \in \mathcal{B} \\ c \neq b}} \sum_{k_c \in \mathcal{U}_c} w_{k_c} [\mathbf{H}_{c,b}^H \mathbf{F}_c^{RF} (\mathbf{R}_{k_c}^{-1} - \mathbf{R}_{k_c}^{-1} + \beta_c \text{diag}(\mathbf{R}_{k_c}^{-1} - \mathbf{R}_{k_c}^{-1})) \mathbf{F}_c^{RFH} \mathbf{H}_{c,b} + k_b \text{diag}(\mathbf{H}_{c,b}^H \mathbf{F}_c^{RF} (\mathbf{R}_{k_c}^{-1} - \mathbf{R}_{k_c}^{-1}) \mathbf{F}_c^{RFH} \mathbf{H}_{c,b})]$
$\hat{\mathbf{G}}_{j_b,\bar{b}}^{DL}$	$\sum_{\substack{c \in \mathcal{B} \\ c \neq b}} \sum_{j_c \in \mathcal{D}_c} w_{j_c} [\mathbf{H}_{j_c,b}^H (\mathbf{R}_{j_c}^{-1} - \mathbf{R}_{j_c}^{-1} + \beta_{j_c} \text{diag}(\mathbf{R}_{j_c}^{-1} - \mathbf{R}_{j_c}^{-1})) \mathbf{H}_{j_c,b} + k_b \text{diag}(\mathbf{H}_{j_c,b}^H (\mathbf{R}_{j_c}^{-1} - \mathbf{R}_{j_c}^{-1}) \mathbf{H}_{j_c,b})]$

concave in  $\mathbf{Q}_{j_b}$  and  $\text{WSR}_{j_b}^{DL}$ ,  $\text{WSR}_b^{UL}$ ,  $\text{WSR}_{\bar{b}}^{UL}$ ,  $\text{WSR}_{\bar{b}}^{DL}$  are non concave in  $\mathbf{Q}_{j_b}$ . As a linear function is simultaneously convex and concave, DC programming introduces the first order Taylor series expansion of  $\text{WSR}_{k_b}^{UL}$ ,  $\text{WSR}_b^{DL}$ ,  $\text{WSR}_{\bar{b}}^{UL}$  and  $\text{WSR}_{\bar{b}}^{DL}$  in  $\mathbf{T}_{k_b}$ , around  $\hat{\mathbf{T}}_{k_b}$  (i.e. around all  $\mathbf{T}_{k_b}$ ), and for  $\text{WSR}_{j_b}^{DL}$ ,  $\text{WSR}_b^{UL}$ ,  $\text{WSR}_{\bar{b}}^{UL}$ ,  $\text{WSR}_{\bar{b}}^{DL}$  around  $\hat{\mathbf{Q}}_{j_b}$  (i.e. around all  $\mathbf{Q}_{j_b}$ ). Let  $\hat{\mathbf{T}}$  and  $\hat{\mathbf{Q}}$  denote the sets containing all such  $\hat{\mathbf{T}}_{k_b}$  and  $\hat{\mathbf{Q}}_{j_b}$ , respectively. The tangent expressions with respect to the non-concave terms for  $\mathbf{T}_{k_b}$  can be written by computing the following gradients

$$\hat{\mathbf{G}}_{k_b,b}^{UL} = -\frac{\partial \text{WSR}_{k_b}^{UL}}{\partial \mathbf{T}_{k_b}} \Big|_{\hat{\mathbf{T}}, \hat{\mathbf{Q}}}, \hat{\mathbf{G}}_{k_b,b}^{DL} = -\frac{\partial \text{WSR}_b^{DL}}{\partial \mathbf{T}_{k_b}} \Big|_{\hat{\mathbf{T}}, \hat{\mathbf{Q}}}, \hat{\mathbf{G}}_{k_b,\bar{b}}^{UL} = -\frac{\partial \text{WSR}_{\bar{b}}^{UL}}{\partial \mathbf{T}_{k_b}} \Big|_{\hat{\mathbf{T}}, \hat{\mathbf{Q}}}, \hat{\mathbf{G}}_{k_b,\bar{b}}^{DL} = -\frac{\partial \text{WSR}_{\bar{b}}^{DL}}{\partial \mathbf{T}_{k_b}} \Big|_{\hat{\mathbf{T}}, \hat{\mathbf{Q}}}, \quad (11)$$

which allow to write the following minorizers  $\underline{\text{WSR}}_{k_b}^{UL}$ ,  $\underline{\text{WSR}}_b^{DL}$ ,  $\underline{\text{WSR}}_{\bar{b}}^{UL}$  and  $\underline{\text{WSR}}_{\bar{b}}^{DL}$  with respect to  $\mathbf{T}_{k_b}$ . Similarly, for the transmit covariance matrix  $\mathbf{Q}_{j_b}$ , we have the gradients

$$\hat{\mathbf{G}}_{j_b,b}^{UL} = -\frac{\partial \text{WSR}_b^{UL}}{\partial \mathbf{Q}_{j_b}} \Big|_{\hat{\mathbf{T}}, \hat{\mathbf{Q}}}, \hat{\mathbf{G}}_{j_b,b}^{DL} = -\frac{\partial \text{WSR}_{j_b}^{DL}}{\partial \mathbf{Q}_{j_b}} \Big|_{\hat{\mathbf{T}}, \hat{\mathbf{Q}}}, \hat{\mathbf{G}}_{j_b,\bar{b}}^{UL} = -\frac{\partial \text{WSR}_{\bar{b}}^{UL}}{\partial \mathbf{Q}_{j_b}} \Big|_{\hat{\mathbf{T}}, \hat{\mathbf{Q}}}, \hat{\mathbf{G}}_{j_b,\bar{b}}^{DL} = -\frac{\partial \text{WSR}_{\bar{b}}^{DL}}{\partial \mathbf{Q}_{j_b}} \Big|_{\hat{\mathbf{T}}, \hat{\mathbf{Q}}}, \quad (12a)$$

which allow to write the minorizers  $\underline{\text{WSR}}_b^{UL}$ ,  $\underline{\text{WSR}}_{j_b}^{DL}$ ,  $\underline{\text{WSR}}_{\bar{b}}^{UL}$  and  $\underline{\text{WSR}}_{\bar{b}}^{DL}$  with respect to  $\mathbf{Q}_{j_b}$ . The gradients (11) and (12) can be computed by applying the matrix differentiation properties and the result Lemma 3 [20], and they are reported in Table I. We remark that the tangent expressions constitute a touching lower bound for the original WSR cost function. Hence, the DC programming approach is also a MM approach, regardless of the restatement of the transmit covariance matrices  $\mathbf{T}_{k_b}$  and  $\mathbf{Q}_{j_b}$  as a function of the beamformers.

Let  $\lambda_{k_b}$  and  $\psi_b$  denote the Lagrange multipliers associated with the sum-power constraint for UL user  $k_b \in \mathcal{U}_b$  and FD BS  $b \in \mathcal{B}$ , respectively. Hereafter, for notational convenience, we define the following matrices

$$\mathbf{H}_{k_b}^H \mathbf{F}_b^{RF} \mathbf{R}_{k_b}^{-1} \mathbf{F}_b^{RFH} \mathbf{H}_{k_b} = \boldsymbol{\Sigma}_{k_b}^1, \quad \hat{\mathbf{G}}_{k_b,b}^{UL} + \hat{\mathbf{G}}_{k_b,b}^{DL} + \hat{\mathbf{G}}_{k_b,\bar{b}}^{UL} + \hat{\mathbf{G}}_{k_b,\bar{b}}^{DL} + \lambda_{k_b} \mathbf{I} = \boldsymbol{\Sigma}_{k_b}^2, \quad (13a)$$

$$\mathbf{H}_{j_b}^H \mathbf{R}_{j_b}^{-1} \mathbf{H}_{j_b} = \boldsymbol{\Sigma}_{j_b}^1, \quad \hat{\mathbf{G}}_{j_b,b}^{UL} + \hat{\mathbf{G}}_{j_b,b}^{DL} + \hat{\mathbf{G}}_{j_b,\bar{b}}^{UL} + \hat{\mathbf{G}}_{j_b,\bar{b}}^{DL} + \psi_b \mathbf{I} = \boldsymbol{\Sigma}_{j_b}^2. \quad (13b)$$

By considering the minorized WSR constructed with the gradients (11)-(12), ignoring the constant terms and the unit-modulus and quantization constraints (9d), and augmenting the minorized WSR only with the sum-power constraints leads to the following Lagrangian

$$\begin{aligned} \mathcal{L} = & \sum_{b \in \mathcal{B}} \sum_{k_b \in \mathcal{U}_b} [w_{k_b} \ln \det(\mathbf{I} + \mathbf{U}_{k_b}^H \boldsymbol{\Sigma}_{k_b}^1 \mathbf{U}_{k_b}) - \text{Tr}(\mathbf{U}_{k_b}^H \boldsymbol{\Sigma}_{k_b}^2 \mathbf{U}_{k_b}) + \lambda_{k_b} p_{k_b}] \\ & + \sum_{b \in \mathcal{B}} \left( \sum_{j_b \in \mathcal{D}_b} [w_{j_b} \ln \det(\mathbf{I} + \mathbf{V}_{j_b}^H \mathbf{G}_b^{RFH} \boldsymbol{\Sigma}_{j_b}^1 \mathbf{G}_b^{RF} \mathbf{V}_{j_b}) - \text{Tr}(\mathbf{V}_{j_b}^H \mathbf{G}_b^{RFH} \boldsymbol{\Sigma}_{j_b}^2 \mathbf{G}_b^{RF} \mathbf{V}_{j_b})] + \psi_b p_b \right). \end{aligned} \quad (14)$$

We note that the constraints on the analog part, omitted in (14), will be incorporated later.

#### IV. CENTRALIZED HYBRID BEAMFORMING

This section presents a novel C-HYBF design based on alternating optimization to solve (14) to a local optimum. Hereafter, different sub-sections are dedicated for the optimization of different variables and at each step complete information of the other variables is summarized in the gradients, which are updated at each iteration.

##### A. Digital Beamforming

To optimize the digital beamformers  $\mathbf{U}_{k_b}$  and  $\mathbf{V}_{j_b}$  we take the derivatives of (14) with respect to their conjugates, which yield the following Karush–Kuhn–Tucker (KKT) conditions

$$\boldsymbol{\Sigma}_{k_b}^1 \mathbf{U}_{k_b} (\mathbf{I} + \mathbf{U}_{k_b}^H \boldsymbol{\Sigma}_{k_b}^1 \mathbf{U}_{k_b})^{-1} - \boldsymbol{\Sigma}_{k_b}^2 \mathbf{U}_{k_b} = 0, \quad (15a)$$

$$\mathbf{G}_b^{RFH} \boldsymbol{\Sigma}_{j_b}^1 \mathbf{G}_b^{RF} \mathbf{V}_{j_b} (\mathbf{I} + \mathbf{V}_{j_b}^H \mathbf{G}_b^{RFH} \boldsymbol{\Sigma}_{j_b}^1 \mathbf{G}_b^{RF} \mathbf{V}_{j_b})^{-1} - \mathbf{G}_b^{RFH} \boldsymbol{\Sigma}_{j_b}^2 \mathbf{G}_b^{RF} \mathbf{V}_{j_b} = 0. \quad (15b)$$

**Theorem 1.** *The WSR maximizing digital beamformers  $\mathbf{U}_{k_b}$  and  $\mathbf{V}_{j_b}$  can be computed as the generalized dominant eigenvector solution of the pair of the following matrices*

$$\mathbf{U}_{k_b} = \mathbf{D}_{d_{k_b}}(\boldsymbol{\Sigma}_{k_b}^1, \boldsymbol{\Sigma}_{k_b}^2), \quad \mathbf{V}_{j_b} = \mathbf{D}_{d_{j_b}}(\mathbf{G}_b^{RFH} \boldsymbol{\Sigma}_{j_b}^1 \mathbf{G}_b^{RF}, \mathbf{G}_b^{RFH} \boldsymbol{\Sigma}_{j_b}^2 \mathbf{G}_b^{RF}), \quad (16)$$

where the matrix  $\mathbf{D}_{d_{k_b}}$  ( $\mathbf{D}_{d_{k_b}}$ ) selects  $d_{k_b}$  ( $d_{k_b}$ ) generalized dominant eigenvectors.

*Proof.* The proof is straightforward by extending the result proved in Theorem 2 [20] for a single-cell mmWave mMIMO FD case, by considering also the linearization terms with respect to the users outside the cell served by FD BS  $b \in \mathcal{B}$ .  $\square$

After optimizing the digital beamformers  $\mathbf{U}_{k_b}$  and  $\mathbf{V}_{j_b}$ , we consider scaling them to unit-norm columns. Such operation preserves the optimized beamforming directions and allows to design the optimal power allocation scheme.

### B. Analog Beamforming

To design the analog beamformer  $\mathbf{G}_b^{RF}$  for FD BS  $b \in \mathcal{B}$ , we assume the remaining variables to be fixed. By considering only the dependence of the WSR on the unconstrained analog beamformer  $\mathbf{G}_b^{RF}$ , we have to solve the following optimization problem

$$\max_{\mathbf{G}_b^{RF}} \sum_{j_b \in \mathcal{D}_b} [w_{j_b} \text{Indet}(\mathbf{I} + \mathbf{V}_{j_b}^H \mathbf{G}_b^{RFH} \boldsymbol{\Sigma}_{j_b}^1 \mathbf{G}_b^{RF} \mathbf{V}_{j_b}) - \text{Tr}(\mathbf{V}_{j_b}^H \mathbf{G}_b^{RFH} \boldsymbol{\Sigma}_{j_b}^2 \mathbf{G}_b^{RF} \mathbf{V}_{j_b})]. \quad (17)$$

We take its derivative with respect to the conjugate of  $\mathbf{G}_b^{RF}$  which leads to the following KKT condition

$$\sum_{j_b \in \mathcal{D}_b} \boldsymbol{\Sigma}_{j_b}^1 \mathbf{G}_b^{RF} \mathbf{V}_{j_b} \mathbf{V}_{j_b}^H (\mathbf{I} + \mathbf{V}_{j_b} \mathbf{V}_{j_b}^H \mathbf{G}_b^{RFH} \boldsymbol{\Sigma}_{j_b}^1 \mathbf{G}_b^{RF})^{-1} - \boldsymbol{\Sigma}_{j_b}^2 \mathbf{G}_b^{RF} \mathbf{V}_{j_b} \mathbf{V}_{j_b}^H = 0. \quad (18)$$

**Theorem 2.** *The vectorized unconstrained analog beamformer  $\mathbf{G}_b^{RF}$  which is common to all the DL users in set  $\mathcal{D}_b$ , can be optimized as one generalized dominant eigenvector solution of the pair of the sum of following matrices*

$$\text{vec}(\mathbf{G}_b^{RF}) = \mathbf{D}_1 \left( \sum_{j_b \in \mathcal{D}_b} (\mathbf{V}_{j_b} \mathbf{V}_{j_b}^H (\mathbf{I} + \mathbf{V}_{j_b} \mathbf{V}_{j_b}^H \mathbf{G}_b^{RFH} \boldsymbol{\Sigma}_{j_b}^1 \mathbf{G}_b^{RF})^{-1})^T \otimes \boldsymbol{\Sigma}_{j_b}^1, \sum_{j_b \in \mathcal{D}_b} (\mathbf{V}_{j_b} \mathbf{V}_{j_b}^H)^T \otimes (\boldsymbol{\Sigma}_{j_b}^2) \right). \quad (19)$$

*Proof.* The proof follows directly from the proof of Theorem 3 [20] for a single-cell by considering also the linearization terms with respect to the users outside the cell.  $\square$

The result stated in Theorem 2 provides the optimized vectorized unconstrained analog beamformer. Operation  $\text{unvec}(\text{vec}(\mathbf{G}_b^{RF}))$  is required to reshape it into correct dimensions, and to meet the unit-modulus and quantization constraints, we preserve only the phase part with the operator  $\angle \cdot$  and pass it through the quantizer such that  $\mathbf{G}_b^{RF} = \mathbb{Q}_b(\angle \mathbf{G}_b^{RF}(m, n)) \in \mathcal{P}_b, \forall m, n$ .

### C. Analog Combining

Optimization of the analog combiner  $\mathbf{F}_b^{RF}$  is straightforward compared to the analog beamformer. Note that the analog combiners do not appear in the trace operators of (14) as they do not generate any interference towards other links. Therefore, to optimize  $\mathbf{F}_b^{RF}$  we can directly consider the original problem (9) which is purely concave with respect to  $\mathbf{F}_b^{RF}$ .

The objective of the analog combiner  $\mathbf{F}_b^{RF}$  is to combine the received covariance matrices at the antenna level such that the WSR is maximized. Let  $(\mathbf{R}_{k_b}^a)$   $\mathbf{R}_{k_b}^a$  denote the (signal plus) interference and noise covariance matrices received at the antennas of the FD BS  $b \in \mathcal{B}$  to be combined with  $\mathbf{F}_b^{RF}$ . Given  $\mathbf{R}_{k_b}^a$  and  $\mathbf{R}_{\bar{k}_b}^a$ , the matrices  $\mathbf{R}_{k_b}$  and  $\mathbf{R}_{\bar{k}_b}$  can be recovered as  $\mathbf{R}_{k_b} = \mathbf{F}_b^{RFH} \mathbf{R}_{k_b}^a \mathbf{F}_b^{RF}$  and  $\mathbf{R}_{\bar{k}_b} = \mathbf{F}_b^{RFH} \mathbf{R}_{\bar{k}_b}^a \mathbf{F}_b^{RF}$ . Problem (9), with respect to the unconstrained analog combiner  $\mathbf{F}_b^{RF}$ , by using the properties of the logarithm function can be restated as

$$\max_{\mathbf{F}_b^{RF}} \sum_{k_b \in \mathcal{U}_b} w_{k_b} [\text{Indet}(\mathbf{F}_b^{RFH} \mathbf{R}_{k_b}^a \mathbf{F}_b^{RF}) - \text{Indet}(\mathbf{F}_b^{RFH} \mathbf{R}_{\bar{k}_b}^a \mathbf{F}_b^{RF})]. \quad (20)$$

Solving (20), which is purely concave, leads to the following optimal analog combiner

$$\mathbf{F}_b^{RF} = \mathbf{D}_{N_b^{RF}} \left( \sum_{k_b \in \mathcal{U}_b} w_{k_b} \mathbf{R}_{k_b}^a, \sum_{k_b \in \mathcal{U}_b} w_{k_b} \mathbf{R}_{\bar{k}_b}^a \right), \quad (21)$$

where the matrix  $\mathbf{D}_{N_b^{RF}}$  selects dominant generalized eigenvectors equal to the number of receive RF chains  $N_b^{RF}$  at the FD BS  $b \in \mathcal{B}$ . To meet the constraints for (21), we normalize its amplitudes with the operator  $\angle \cdot$  and pass it through the quantizer such that  $\mathbf{F}_b^{RF} = \mathbb{Q}_b(\angle \mathbf{F}_b^{RF}(m, n)) \in \mathcal{P}_b$ .

### D. Optimal Power Allocation

Let  $\mathbf{P}_{k_b}$  and  $\mathbf{P}_{j_b}$  denote the stream power matrices for the UL user  $k_b \in \mathcal{U}_b$  and DL user  $j_b \in \mathcal{D}_b$ , respectively. Given the normalized digital beamformers with the unit-norm columns (16), the power allocation problems for  $\mathbf{P}_{k_b}$  and  $\mathbf{P}_{j_b}$  can be formally stated as

$$\max_{\mathbf{P}_{k_b}} [w_{k_b} \text{Indet}(\mathbf{I} + \mathbf{U}_{k_b}^H \boldsymbol{\Sigma}_{k_b}^1 \mathbf{U}_{k_b} \mathbf{P}_{k_b}) - \text{Tr}(\mathbf{U}_{k_b}^H \boldsymbol{\Sigma}_{k_b}^2 \mathbf{U}_{k_b} \mathbf{P}_{k_b})], \quad (22a)$$

$$\max_{\mathbf{P}_{j_b}} [w_{j_b} \text{Indet}(\mathbf{I} + \mathbf{V}_{j_b}^H \mathbf{G}_b^{RFH} \boldsymbol{\Sigma}_{j_b}^1 \mathbf{G}_b^{RF} \mathbf{V}_{j_b} \mathbf{P}_{j_b}) - \text{Tr}(\mathbf{V}_{j_b}^H \mathbf{G}_b^{RFH} \boldsymbol{\Sigma}_{j_b}^2 \mathbf{G}_b^{RF} \mathbf{V}_{j_b} \mathbf{P}_{j_b})], \quad (22b)$$

and solving them leads to the following optimal power allocation scheme

$$\mathbf{P}_{k_b} = (w_{k_b} (\mathbf{U}_{k_b}^H \boldsymbol{\Sigma}_{k_b}^2 \mathbf{U}_{k_b})^{-1} - (\mathbf{U}_{k_b}^H \boldsymbol{\Sigma}_{k_b}^1 \mathbf{U}_{k_b})^{-1})^+, \quad (23a)$$

$$\mathbf{P}_{j_b} = (w_{j_b} (\mathbf{V}_{j_b}^H \mathbf{G}_b^{RFH} \boldsymbol{\Sigma}_{j_b}^2 \mathbf{G}_b^{RF} \mathbf{V}_{j_b})^{-1} - (\mathbf{V}_{j_b}^H \mathbf{G}_b^{RFH} \boldsymbol{\Sigma}_{j_b}^1 \mathbf{G}_b^{RF} \mathbf{V}_{j_b})^{-1})^+, \quad (23b)$$

where  $(\mathbf{X})^+ = \max\{\mathbf{0}, \mathbf{X}\}$ . Given the optimal stream powers, we can search for the Lagrange multipliers satisfying the total sum-power constraint. Let  $\mathbf{P}^{DL}$  and  $\mathbf{P}^{UL}$  denote the collection of powers in DL and UL, respectively, and let  $\mathbf{\Lambda}$  and  $\mathbf{\Psi}$  denote the collection of multipliers for  $\lambda_{k_b}$  and  $\psi_b$ , respectively. Given (23), consider the dependence of the Lagrangian only on the multipliers and powers as  $\mathcal{L}(\mathbf{\Lambda}, \mathbf{\Psi}, \mathbf{P}^{DL}, \mathbf{P}^{UL})$ , obtained by including the power matrices  $\mathbf{P}_{k_b}$  and  $\mathbf{P}_{j_b}$  in (14).

The multipliers in  $\mathbf{\Lambda}$  and  $\mathbf{\Psi}$  should be such that the Lagrangian is finite and the values of multipliers are strictly positive, i.e.,

$$\begin{aligned} \min_{\mathbf{\Psi}, \mathbf{\Lambda}} \max_{\mathbf{P}^{DL}, \mathbf{P}^{UL}} \mathcal{L}(\mathbf{\Lambda}, \mathbf{\Psi}, \mathbf{P}^{DL}, \mathbf{P}^{UL}), \\ \text{s.t.} \quad \mathbf{\Psi}, \mathbf{\Lambda} \geq 0. \end{aligned} \quad (24)$$

The dual function

$$\max_{\mathbf{P}^{DL}, \mathbf{P}^{UL}} \mathcal{L}(\mathbf{\Lambda}, \mathbf{\Psi}, \mathbf{P}^{DL}, \mathbf{P}^{UL})$$

is the pointwise supremum of a family of functions of  $\mathbf{\Psi}, \mathbf{\Lambda}$ , it is convex [31] and the globally optimal values for  $\mathbf{\Psi}$  and  $\mathbf{\Lambda}$  can be found by using any of the numerous convex-optimization techniques. In this work, the Bisection method is adopted. Let  $\underline{\lambda}_{k_b}, \underline{\psi}_b$  and  $\overline{\psi}_b, \overline{\lambda}_{k_b}$  denote the upper and lower bounds for searching the multipliers  $\psi_b$  and  $\lambda_{k_b}$ , respectively, and let  $[0, \lambda_{k_b}^{max}]$  and  $[0, \psi_b^{max}]$  denote their search range. As the generalized dominant eigenvector solution is computed given fixed multipliers, doing water-filling for the powers while searching for the multipliers leads to non diagonal power matrices. Hence, consider a SVD of the powers as  $[\mathbf{L}_{\mathbf{P}_i}^{svd}, \mathbf{D}_{\mathbf{P}_i}^{svd}, \mathbf{R}_{\mathbf{P}_i}^{svd}] = \text{svd}(\mathbf{P}_i)$ , with  $\mathbf{P}_i = \mathbf{P}_{k_b}$  or  $\mathbf{P}_i = \mathbf{P}_{j_b}$ , and the matrices  $\mathbf{L}_{\mathbf{P}_i}^{svd}, \mathbf{D}_{\mathbf{P}_i}^{svd}$  and  $\mathbf{R}_{\mathbf{P}_i}^{svd}$  denote the left unitary, diagonal and right unitary matrices obtained from the SVD of  $\mathbf{P}_i$ . The diagonal structure of the power matrices while searching for the multipliers can be re-established as  $\mathbf{P}_i = \mathbf{D}_i$ , with  $i \in \mathcal{U}_b$  or  $i \in \mathcal{D}_b$ .

By using the closed form expressions derived above, the complete alternating optimization based C-HYBF procedure to solve (9) is formally stated in Algorithm 1.

### E. Convergence of C-HYBF

The convergence of Algorithm 1 can be proved by using the minorization theory [30], alternating or cyclic optimization [30], Lagrange dual function [31], saddle-point interpretation [31] and KKT conditions [31]. For the WSR cost function (9), we construct its minorizer, which is a touching lower bound for (9), hence we can write

---

**Algorithm 1** Centralized Hybrid Beamforming
 

---

**Given:** The CSI and rate weights.

**Initialize:**  $\mathbf{G}_b^{RF}, \mathbf{F}_b^{RF}, \mathbf{V}_{j_b}, \mathbf{U}_{k_b}, \forall j_b \text{ \& \; } \forall k_b$ .

**Set:**  $\lambda_{k_b} = 0, \overline{\lambda_{k_b}} = \lambda_{k_b}^{max}, \psi_b = 0, \overline{\psi_b} = \psi_b^{max}, \forall k_b \text{ \& \; } \forall b$

**Repeat until convergence**

**for**  $b = 1 : B$

Compute  $\mathbf{G}_b^{RF}$  with (19), do  $\text{unvec}(\mathbf{G}_b^{RF})$  and get  $\angle \mathbf{G}_t$

**for:**  $j_b = 1 : D_b$

Compute  $\hat{\mathbf{G}}_{j_b,b}^{UL}, \hat{\mathbf{G}}_{j_b,b}^{DL}, \hat{\mathbf{G}}_{j_b,\bar{b}}^{UL}, \hat{\mathbf{G}}_{j_b,\bar{b}}^{DL}$  from Table I, optimize  $\mathbf{V}_{j_b}$  with (16) and normalize its columns

Next  $j_b$

**Repeat until convergence**

set  $\psi_b = (\underline{\psi_b} + \overline{\psi_b})/2$

**for**  $j_b = 1 : D_b$

Compute  $\mathbf{P}_{j_b}$  with (23), do SVD, set  $\mathbf{P}_{j_b} = \mathbf{D}_{P_{j_b}}^{svd}$  and finally set  $\mathbf{Q}_{j_b} = \mathbf{G}_b \mathbf{V}_{j_b} \mathbf{P}_{j_b} \mathbf{V}_{j_b}^H \mathbf{G}_b^H$

Next  $j_b$

**if** constraint for  $\psi_b$  is violated

set  $\underline{\psi_b} = \psi_b$ ,

**else**  $\overline{\psi_b} = \psi_b$

**for:**  $k_b = 1 : K_b$

Compute  $\hat{\mathbf{G}}_{k_b,b}^{UL}, \hat{\mathbf{G}}_{k_b,b}^{DL}, \hat{\mathbf{G}}_{k_b,\bar{b}}^{UL}, \hat{\mathbf{G}}_{k_b,\bar{b}}^{DL}$  from Table I, optimize  $\mathbf{U}_{k_b}$  with (16) and normalize its columns

**Repeat until convergence**

set  $\lambda_{k_b} = (\underline{\lambda_{k_b}} + \overline{\lambda_{k_b}})/2$

Compute  $\mathbf{P}_{k_b}$  with (23), do SVD, set  $\mathbf{P}_{k_b} = \mathbf{D}_{P_{k_b}}^{svd}$  and finally set  $\mathbf{T}_b = \mathbf{U}_{k_b} \mathbf{P}_{k_b} \mathbf{U}_{k_b}^H$

**if** constraint for  $\lambda_{k_b}$  is violated

set  $\underline{\lambda_{k_b}} = \lambda_{k_b}$

**else**  $\overline{\lambda_{k_b}} = \lambda_{k_b}$

Next  $k_b$

Next  $b$

**Quantize**  $\mathbf{G}_b^{RF}$  and  $\mathbf{F}_b^{RF}$ , with  $\mathbb{Q}_b(\cdot), \forall b$

---

$$\text{WSR} \geq \underline{\text{WSR}} = \underline{\text{WR}}_{k_b,b}^{UL} + \underline{\text{WSR}}_{k_b,b}^{UL} + \underline{\text{WR}}_{j_b,b}^{DL} + \underline{\text{WSR}}_{j_b,b}^{DL} + \underline{\text{WSR}}_b^{DL} + \underline{\text{WSR}}_b^{UL}. \quad (25)$$

The minorized WSR, which is concave in  $\mathbf{T}_{k_b}$  and  $\mathbf{Q}_{j_b}$ , has the same gradient of the original WSR maximization problem (9), hence the KKT conditions are not affected. Reparameterizing  $\mathbf{T}_{k_b}$  or  $\mathbf{Q}_{j_b}$  in terms of  $\mathbf{G}_b^{RF}, \mathbf{V}_{j_b}, \forall j_b \in \mathcal{D}_b$ , or  $\mathbf{U}_{k_b}, \forall k_b \in \mathcal{U}_b$ , respectively, augmenting the minorized WSR cost function with the Lagrange multipliers and power constraints leads to (14).

By incorporating further the power matrices we get to  $\mathcal{L}(\mathbf{\Lambda}, \mathbf{\Psi}, \mathbf{P}^{DL}, \mathbf{P}^{UL})$ . Every alternating update of the  $\mathcal{L}$  for the variables  $\mathbf{G}_b^{RF}, \mathbf{F}_b^{RF}, \forall b \in \mathcal{B}, \mathbf{V}_{j_b}, \forall j_b \in \mathcal{D}_b, \mathbf{U}_{k_b}, \forall k_b \in \mathcal{U}_b, \mathbf{P}_{k_b}, \mathbf{P}_{j_b}, \lambda_{k_b}$  and  $\psi_b$ , leads to a monotonic increase of the WSR, which assures convergence. For the KKT conditions, at the convergence point, the gradients of  $\mathcal{L}$  for  $\mathbf{V}_{j_b}, \mathbf{G}_b^{RF}, \mathbf{U}_{k_b}$  or  $\mathbf{P}_{k_b}, \mathbf{P}_{j_b}$  correspond to the gradients of the Lagrangian of the original problem (9), and hence the sub-optimal solution for the minorized WSR matches the sub-optimal solution of the original problem. For the fixed analog and digital beamformers,  $\mathcal{L}$  is concave in powers, hence we have strong duality for the saddle point, i.e.,

$$\max_{\mathbf{P}^{DL}, \mathbf{P}^{UL}} \min_{\mathbf{\Lambda}, \mathbf{\Psi}} \mathcal{L}(\mathbf{\Lambda}, \mathbf{\Psi}, \mathbf{P}^{UL}, \mathbf{P}^{DL}). \quad (26)$$

Let  $\mathbf{X}^*$  and  $x^*$  denote the optimal solution for matrix  $\mathbf{X}$  or scalar  $x$  at the convergence, respectively. As each iteration leads to a monotonic increase in the WSR and the power are updated by satisfying the sum-power constraint, at the convergence point, the solution of the optimization problem

$$\min_{\mathbf{\Lambda}, \mathbf{\Psi}} \mathcal{L}(\mathbf{V}_{j_b}^*, \mathbf{G}_b^{RF*}, \mathbf{F}_b^{RF*}, \mathbf{U}_b^{RF*}, \mathbf{P}^{DL*}, \mathbf{P}^{UL*}, \mathbf{\Lambda}, \mathbf{\Psi}) \quad (27)$$

satisfies the KKT conditions for the powers in  $\mathbf{P}^{DL}$  and  $\mathbf{P}^{UL}$  and the complementary slackness conditions

$$\psi_b^* (p_b - \sum_{j_b \in \mathcal{D}_b} \text{Tr}(\mathbf{G}_b^{RF*} \mathbf{V}_{j_b}^* \mathbf{P}_{j_b}^* \mathbf{V}_{j_b}^{*H} \mathbf{G}_b^{RF*H})) = 0, \quad \lambda_{k_b}^* (p_{k_b} - \text{Tr}(\mathbf{U}_{k_b}^* \mathbf{P}_{k_b}^* \mathbf{U}_{k_b}^{*H})) = 0, \quad (28a)$$

with the individual factors in the products being non-negative.

## V. PARALLEL AND DISTRIBUTED IMPLEMENTATION

As well-discussed in Section I, implementation of Algorithm 1 in a real-time FD network is infeasible in practice as it requires centralized implementation. To overcome its drawbacks, we present the concept of P&D-HYBF for mmWave based on cooperation. Such design enables per-link independent optimization of the beamformers for each FD BS, thus avoiding full CSI exchange with the central node every CCT and reducing the communication overhead considerably.

To proceed, we assume the following:

- 1) the FD BSs cooperate by exchanging information about the digital beamformers, analog beamformers and analog combiners via a feedback link;
- 2) local CSI is accessible by the FD BSs;

- 3) each FD BS has multiple computational processors dedicated for UL and DL;
- 4) the computations take place at the FD BSs in each cell, in a synchronized manner.

Recall that the MM optimization technique allowed to write the Lagrangian of the original WSR problem (9) as (14) from which it is evident that to update the beamformers for each user at each iteration, only its gradients are required. Therefore, they summarize complete information about all the remaining interfering links in the network. From a practical point-of-view, the gradients for each link take into account the interference generated towards all the other links, and hence limit greedy behaviour. However, (14) is coupled among different links as the covariance matrices of other users directly appear in the gradients, which vary at the update of each beamformer.

To decouple (14) into local per-link independent optimization sub-problems, we assume that each FD BS has some memory to save information. Hereafter, overline will emphasize that the variables are only local and saved in the memory. We introduce the following local variables

$$\overline{\mathbf{L}}_{k_b}^{In} = \hat{\mathbf{G}}_{k_b,b}^{UL} + \hat{\mathbf{G}}_{k_b,b}^{DL}, \quad \overline{\mathbf{L}}_{k_b}^{Out} = \hat{\mathbf{G}}_{k_b,\bar{b}}^{UL} + \hat{\mathbf{G}}_{k_b,\bar{b}}^{DL}, \quad \overline{\mathbf{L}}_{j_b}^{In} = \hat{\mathbf{G}}_{j_b,b}^{UL} + \hat{\mathbf{G}}_{j_b,b}^{DL}, \quad \overline{\mathbf{L}}_{j_b}^{Out} = \hat{\mathbf{G}}_{j_b,\bar{b}}^{UL} + \hat{\mathbf{G}}_{j_b,\bar{b}}^{DL}, \quad (29)$$

to be saved in the memory of FD BS  $b \in \mathcal{B}$ ,  $\forall k_b$  and  $\forall j_b$ . The local variables  $\overline{\mathbf{L}}_{k_b}^{In}$  and  $\overline{\mathbf{L}}_{k_b}^{Out}$  save information about the overall interference generated inside and outside the cell by the beamformer of UL user  $k_b \in \mathcal{U}_b$ , respectively. Similarly, the local variables  $\overline{\mathbf{L}}_{j_b}^{In}$  and  $\overline{\mathbf{L}}_{j_b}^{Out}$  save information about the interference generated in the same cell and in the neighbouring cells by the FD BS  $b \in \mathcal{B}$ , respectively, while serving its DL user  $j_b \in \mathcal{D}_b$ . Note that each FD BS can update the in-cell local variables  $\overline{\mathbf{L}}_{k_b}^{In}$  and  $\overline{\mathbf{L}}_{j_b}^{In}$  by itself. A feedback from the neighboring BSs is required only to update the out-cell variables  $\overline{\mathbf{L}}_{k_b}^{Out}$  and  $\overline{\mathbf{L}}_{j_b}^{Out}$ . To save information about the interference-plus-noise covariance matrices at the RF chains and antenna level (for the analog combiner), we define the following local variables

$$\overline{\mathbf{R}}_{j_b}^{-1} = \mathbf{R}_{j_b}^{-1}, \quad \forall j_b, \quad \text{and} \quad \overline{\mathbf{R}}_{k_b}^{-1} = \mathbf{R}_{k_b}^{-1}, \quad \overline{\mathbf{R}}_{k_b}^a = \mathbf{R}_{k_b}^a, \quad \overline{\mathbf{R}}_{k_b}^a = \mathbf{R}_{k_b}^a, \quad \forall k_b. \quad (30)$$

For notational compactness, similar to (13), we also define the following variables

$$\mathbf{H}_{k_b}^H \mathbf{F}_b^{RF} \overline{\mathbf{R}}_{k_b}^{-1} \mathbf{F}_b^{RFH} \mathbf{H}_{k_b} = \mathbf{Z}_{k_b}^1, \quad \overline{\mathbf{L}}_{k_b}^{In} + \overline{\mathbf{L}}_{k_b}^{out} + \lambda_{k_b} \mathbf{I} = \mathbf{Z}_{k_b}^2, \quad \forall k_b, \quad (31a)$$

$$\mathbf{H}_{j_b}^H \overline{\mathbf{R}}_{j_b}^{-1} \mathbf{H}_{j_b} = \mathbf{Z}_{j_b}^1, \quad \overline{\mathbf{L}}_{j_b}^{In} + \overline{\mathbf{L}}_{j_b}^{out} + \psi_b \mathbf{I} = \mathbf{Z}_{j_b}^2, \quad \forall j_b, \quad (31b)$$



now function only of the fixed local variables. By replacing the gradients with the fixed local variables, the Lagrangian (14) can be rewritten as

$$\begin{aligned} \mathcal{L} = & \sum_{b \in \mathcal{B}} \left( \sum_{k_b \in \mathcal{U}_b} [w_{k_b} \text{Indet}(\mathbf{I} + \mathbf{U}_{k_b}^H \mathbf{Z}_{k_b}^1 \mathbf{U}_{k_b}) - \text{Tr}(\mathbf{U}_{k_b}^H \mathbf{Z}_{k_b}^2 \mathbf{U}_{k_b}) + \lambda_{k_b} p_{k_b}] \right. \\ & \left. + \sum_{j_b \in \mathcal{D}_b} [w_{j_b} \text{Indet}(\mathbf{I} + \mathbf{V}_{j_b}^H \mathbf{G}_b^{RFH} \mathbf{Z}_{j_b}^1 \mathbf{G}_b^{RF} \mathbf{V}_{j_b}) - \text{Tr}(\mathbf{V}_{j_b}^H \mathbf{G}_b^{RFH} (\mathbf{Z}_{j_b}^1 \mathbf{G}_b^{RF} \mathbf{V}_{j_b}))] + \psi_b p_b \right). \end{aligned} \quad (32)$$

In contrast to (14), (32) becomes fully decoupled as it is a function only of the local variables, which are fixed. However, note that in UL and DL, the optimization of the analog combiner  $\mathbf{F}_b^{RF}$  and analog beamformer  $\mathbf{G}_b^{RF}$ ,  $\forall b \in \mathcal{B}$ , is still coupled as they are common among the UL and DL users in the same cell, respectively. Moreover, the analog beamformer  $\mathbf{G}_b^{RF}$  also affects the total transmit power of each FD BS, posing a serious challenge for enabling per-link independent optimization in DL from (32). Handling of the coupling constraints and P&D optimization for HYBF from (32) is presented in the following.

#### A. Per-Link Independent Sub-Problems in UL

Each UL user has its own sum-power constraint but the analog combiner  $\mathbf{F}_b^{RF}$ , appearing in  $\mathbf{Z}_{k_b}^1$ , is common among all the UL users in the same cell. To decouple their optimization, we assume that FD BS  $b \in \mathcal{B}$  updates  $\mathbf{F}_b^{RF}$  only after updating all the digital beamformers  $\mathbf{U}_{k_b}$ ,  $\forall k_b \in \mathcal{U}_b$ . Given this assumption and fixed local variables, UL WSR maximization problem for each FD BS reduces into three layers of sub-problems. At the bottom layer, FD BS  $b \in \mathcal{B}$  has to solve independent sub-problems to update  $\mathbf{U}_{k_b}$ , whose optimization is fully decoupled and therefore can be done in parallel  $\forall k_b$ . At the middle layer, FD BS  $b \in \mathcal{B}$  has to independently update the stream power matrix  $\mathbf{P}_{k_b}$  while searching the multiplier  $\lambda_{k_b}$ ,  $\forall k_b$ . Finally, at the top layer, once the two-layer UL sub-problems are solved, only one update of the analog combiner is required. Fig. 3 highlights the idea of the proposed per-link decomposition for the UL WSR for FD BS  $b \in \mathcal{B}$  into three sub-layers, and the sub-problems at each layer must be solved from the bottom to the top.

Due to per-link independent decomposition, the Lagrangian for the UL user  $k_b \in \mathcal{U}_b$  with independent sum-power constraint  $p_{k_b}$  and fixed local variables can be written as

$$\mathcal{L}_{k_b} = w_{k_b} \text{Indet}(\mathbf{I} + \mathbf{U}_{k_b}^H \mathbf{Z}_{k_b}^1 \mathbf{U}_{k_b}) - \text{Tr}(\mathbf{U}_{k_b}^H \mathbf{Z}_{k_b}^2 \mathbf{U}_{k_b}) + \lambda_{k_b} p_{k_b}, \quad (33)$$

in which for the bottom layer the analog combiner  $\mathbf{F}_b^{RF}$  in  $\mathbf{Z}_{k_b}^1$  and the powers are fixed. To optimize  $\mathbf{U}_{k_b}$ , a derivative of (33) can be taken, which leads to a similar KKT condition as

(15a), with  $\Sigma_{k_b}^i$  replaced with  $\mathbf{Z}_{k_b}^i, \forall i$ . By following a similar proof for Theorem 2 [20], it can be easily shown that WSR maximizing  $\mathbf{U}_{k_b}$  for (33) can be computed as

$$\mathbf{U}_{k_b} = \mathbf{D}_{d_{k_b}}(\mathbf{Z}_{k_b}^1, \mathbf{Z}_{k_b}^2). \quad (34)$$

Note that (34) can be computed in parallel by the multi-processor FD BS  $b \in \mathcal{B}, \forall k_b \in \mathcal{U}_b$ .

At the middle layer, the power optimization remains decoupled as each UL user has its own sum-power constraint and the local variables are fixed. To find the optimal  $\mathbf{P}_{k_b}$  in parallel  $\forall k_b$ , we first consider the normalization of the columns of (34) to unit-norm and power allocation problem can be formally stated similar to (22a), but now dependent on the variables  $\mathbf{Z}_{k_b}^i$  instead of  $\Sigma_{k_b}^i, \forall i$ . Solving it independently yields the following parallel power allocation scheme

$$\mathbf{P}_{k_b} = (w_{k_b}(\mathbf{U}_k^H \mathbf{Z}_{k_b}^1 \mathbf{U}_{k_b})^{-1} - (\mathbf{U}_{k_b}^H \mathbf{Z}_{k_b}^2 \mathbf{U}_{k_b})^{-1})^+, \quad (35)$$

which can be computed while searching for the multiplier  $\lambda_{k_b}$  associated with its independent sum-power constraint in parallel  $\forall k_b$ . If  $\mathbf{P}_{k_b}$  becomes non-diagonal, its diagonal structure can be reestablished as  $\mathbf{P}_{k_b} = \mathbf{D}_{\mathbf{P}_{k_b}}^{svd}$ , where  $\mathbf{D}_{\mathbf{P}_{k_b}}^{svd}$  is a diagonal matrix obtained from SVD of the non-diagonal  $\mathbf{P}_{k_b}$ . Multiplier  $\lambda_{k_b}, \forall k_b$ , should be such that (33) is finite and the value of  $\lambda_{k_b}$  should be strictly positive. It can be searched by solving the following problem in parallel

$$\begin{aligned} \min_{\lambda_{k_b}} \max_{\mathbf{P}_{k_b}} \quad & \mathcal{L}_{k_b}(\lambda_{k_b}, \mathbf{P}_{k_b}), \\ \text{s.t.} \quad & \lambda_{k_b} \geq 0, \end{aligned} \quad (36)$$

while independently allocating the powers at the middle layer  $\forall k_b$ . The dual function

$$\max_{\mathbf{P}_{k_b}} \quad \mathcal{L}_{k_b}(\lambda_{k_b}, \mathbf{P}_{k_b}), \quad (37)$$

is convex [31] and can be solved with the Bisection method, as for the C-HYBF scheme.

At the top layer, one update of  $\mathbf{F}_b^{RF}$  is required  $\forall b \in \mathcal{B}$ . Note that simultaneous variation in parallel of the beamformers  $\mathbf{U}_{k_b}$  and powers  $\mathbf{P}_{k_b}, \forall k_b$ , at the bottom and middle layer vary the received covariance matrices, and consequently the information to be updated in the local variables  $\overline{\mathbf{R}}_{k_b}^a$  and  $\overline{\mathbf{R}}_{k_b}^a$  at the antenna level, which  $\mathbf{F}_b^{RF}$  should combine (similar to (21)). As each FD BS  $b \in \mathcal{B}$  has complete information about the optimized variables at the middle and bottom layers, it can use it to update  $\overline{\mathbf{R}}_{k_b}^a$  and  $\overline{\mathbf{R}}_{k_b}^a, \forall k_b \in \mathcal{U}_b$ . As the WSR is fully concave with respect to the analog combiner  $\mathbf{F}_b^{RF}$ , without the constraints and by using the properties of logarithm function, its optimization problem can be stated as

$$\max_{\mathbf{F}_b^{RF}} \sum_{k_b \in \mathcal{U}_b} w_{k_b} [\text{Indet}(\mathbf{F}_b^{RFH} \overline{\mathbf{R}}_{k_b}^a \mathbf{F}_b^{RF}) - \text{Indet}(\mathbf{F}_b^{RFH} \overline{\mathbf{R}}_{k_b}^a \mathbf{F}_b^{RF})], \quad (38)$$

where the local variables have been recently updated by using the information from the middle and bottom layers. Problem (38) is fully concave and solving it leads to the following optimal unconstrained analog combiner

$$\mathbf{F}_b^{RF} = \mathbf{D}_{N_b^{RF}} \left( \sum_{k_b \in \mathcal{U}_b} w_{k_b} \overline{\mathbf{R}}_{k_b}^a, \sum_{k_b \in \mathcal{U}_b} w_{k_b} \overline{\mathbf{R}}_{k_b}^a \right). \quad (39)$$

To meet the unit-modulus and quantization constraints, we normalize its amplitudes with  $\angle \cdot$  to unit-norm and quantize it as  $\mathbf{F}_b^{RF} = \mathbb{Q}_b(\angle \mathbf{F}_b^{RF}) \in \mathcal{P}_b$ .

### B. Per-Link Independent Sub-Problems in DL

Decomposition of the DL WSR is more challenging due to the coupled sum-power constraint among the users in the set  $\mathcal{D}_b, \forall b$ . Moreover,  $\mathbf{G}_b^{RF}$  is also common between the DL users in the same cell and thus affects the total transmit power. To introduce per-link independent decomposition in DL, we assume that each FD BS  $b \in \mathcal{B}$  first updates the digital beamformers for the DL users, while keeping the Lagrange multiplier  $\psi_b$  and the analog beamformer  $\mathbf{G}_b^{RF}$  fixed. Furthermore, the powers are included afterwards, while searching the common multiplier  $\psi_b$ . Given this assumption, the DL WSR problem, for each FD BS  $b \in \mathcal{B}$ , decomposes into three layers of sub-problems. At the bottom layer, each FD BS to update the DL beamformers  $\mathbf{V}_{j_b}$  and normalize its columns to unit-norm, in parallel  $\forall j_b$ . At the middle layer, one update of the analog beamformer  $\mathbf{G}_b^{RF}$  is required. Finally, at the top layer, we have to search for the Lagrange multiplier  $\psi_b$  satisfying the coupled sum-power constraint and update the power matrices  $\mathbf{P}_{j_b}$  for the DL users, in parallel  $\forall j_b$ . Fig. 4 shows the decomposition of the DL WSR into three layers of sub-problems, which must be solved from the bottom to the top.

For FD BS  $b \in \mathcal{B}$ , the Lagrangian for the DL WSR can be written as

$$\mathcal{L}_b^{DL} = \sum_{j_b \in \mathcal{D}_b} w_{j_b} \text{Indet}(\mathbf{I} + \mathbf{V}_{j_b}^H \mathbf{G}_b^{RFH} \mathbf{Z}_{j_b}^1 \mathbf{G}_b^{RF} \mathbf{V}_{j_b}) - \text{Tr}(\mathbf{V}_{j_b}^H \mathbf{G}_b^{RFH} \mathbf{Z}_{j_b}^2 \mathbf{G}_b^{RF} \mathbf{V}_{j_b}) + \psi_b p_b. \quad (40)$$

In (40), for the bottom layer, as  $\psi_b, \mathbf{G}_b^{RF}, \mathbf{Z}_{j_b}^i$  are fixed, optimization of the digital beamformers remains decoupled. To optimize  $\mathbf{V}_{j_b}$  a derivative can be taken, which will lead to a similar KKT condition as (15b), but function of  $\mathbf{Z}_{j_b}^i$  instead of  $\mathbf{\Sigma}_{j_b}^i$ . By following a similar proof for Theorem 2 [20], it can be easily shown that the WSR maximizing  $\mathbf{V}_{j_b}$  can be computed as

$$\mathbf{V}_{j_b} = \mathbf{D}_{d_{j_b}} (\mathbf{G}_b^{RFH} \mathbf{Z}_{j_b}^1 \mathbf{G}_b^{RF}, \mathbf{G}_b^{RFH} \mathbf{Z}_{j_b}^2 \mathbf{G}_b^{RF}). \quad (41)$$

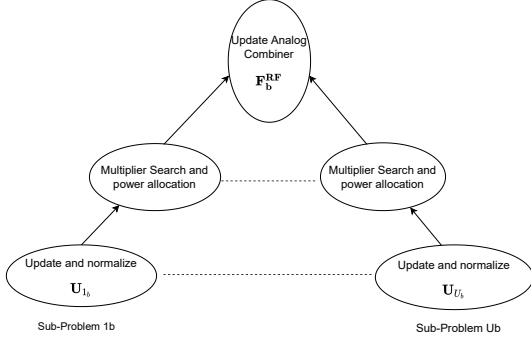


Fig. 3: Decomposition of the UL WSR into three layers of sub-problems  $\forall b \in \mathcal{B}$ .

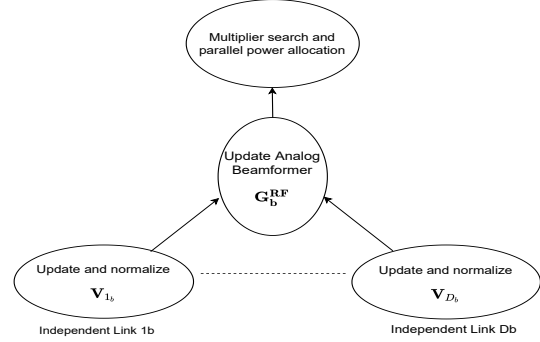


Fig. 4: Decomposition of the DL WSR into three layers of sub-problems  $\forall b \in \mathcal{B}$ .

We consider the normalization of the columns of  $\mathbf{V}_{j_b}$  to unit-norm in parallel  $\forall j_b$ , such that optimal power allocation could be included at the top layer. Once the parallel update of the digital beamformers  $\mathbf{V}_{j_b}, \forall j_b$ , has been made, at the middle layer, FD BS  $b \in \mathcal{B}$  has to optimize the analog combiner  $\mathbf{G}_b^{RF}$ . By considering the unconstrained analog combiner, each FD BS  $b \in \mathcal{B}$  has to independently solve the following optimization problem

$$\max_{\mathbf{G}_b^{RF}} \sum_{j_b \in \mathcal{D}_b} [w_{j_b} \ln \det(\mathbf{I} + \mathbf{V}_{j_b}^H \mathbf{G}_b^{RFH} \mathbf{Z}_{j_b}^1 \mathbf{G}_b^{RF} \mathbf{V}_{j_b}) - \text{Tr}(\mathbf{V}_{j_b}^H \mathbf{G}_b^{RFH} \mathbf{Z}_{j_b}^2 \mathbf{G}_b^{RF} \mathbf{V}_{j_b})]. \quad (42)$$

Note that each FD BS has complete information about the digital beamformers optimized at the bottom layer, which must be first used to update  $\overline{\mathbf{R}}_{j_b}^{-1}$  and  $\overline{\mathbf{L}}_{j_b}^{In}$  appearing in  $\mathbf{Z}_{j_b}^1$  and  $\mathbf{Z}_{j_b}^2$  in (42), respectively,  $\forall j_b$ . To optimize  $\mathbf{G}_b^{RF}$  a derivative of (42) can be taken, which will lead to a similar KKT condition as (18), function of  $\mathbf{Z}_{j_b}^i$  instead of  $\Sigma_{j_b}^i, \forall i$ . By following a similar proof for Theorem 3 [20], it can be easily shown that  $\mathbf{G}_b^{RF}$  can be optimized as

$$\text{vec}(\mathbf{G}_b^{RF}) = \mathbf{D}_1 \left( \sum_{j_b \in \mathcal{D}_b} (\mathbf{V}_{j_b} \mathbf{V}_{j_b}^H (\mathbf{I} + \mathbf{V}_{j_b} \mathbf{V}_{j_b}^H \mathbf{G}_b^{RFH} \mathbf{Z}_{j_b}^1 \mathbf{G}_b^{RF})^{-1})^T \otimes \mathbf{Z}_{j_b}^1, \sum_{j_b \in \mathcal{D}_b} (\mathbf{V}_{j_b} \mathbf{V}_{j_b}^H)^T \otimes \mathbf{Z}_{j_b}^2 \right). \quad (43)$$

The analog combiner  $\mathbf{G}_b^{RF}$  optimized according to (43) is unconstrained and vectorized. Therefore, we do  $\text{unvec}(\text{vec}(\mathbf{G}_b^{RF}))$  to shape it into correct dimensions, normalize the amplitude with  $\angle \cdot$  and quantize it such that  $\mathbf{G}_b^{RF} = \mathbb{Q}(\angle \mathbf{G}_b^{RF}) \in \mathcal{P}_b$ . For the top layer, the optimal stream power allocation can be included while searching the multiplier  $\psi_b$  to satisfy the sum-power constraint  $p_b$ . Assuming the multiplier  $\psi_b$  to be fixed, which is captured in  $\mathbf{Z}_{j_b}^2$ , the power optimization problem  $\forall j_b \in \mathcal{D}_b$  can be stated as

$$\max_{\mathbf{P}_{j_b}} [w_{j_b} \ln \det(\mathbf{I} + \mathbf{V}_{j_b}^H \mathbf{G}_b^{RFH} \mathbf{Z}_{j_b}^1 \mathbf{G}_b^{RF} \mathbf{V}_{j_b} \mathbf{P}_{j_b}) - \text{Tr}(\mathbf{V}_{j_b}^H \mathbf{G}_b^{RFH} \mathbf{Z}_{j_b}^2 \mathbf{G}_b^{RF} \mathbf{V}_{j_b} \mathbf{P}_{j_b})]. \quad (44)$$

In (44), the update of power matrix  $\mathbf{P}_{j_b}, \forall j_b$  remains independent and the multiplier  $\psi_b$  must be updated based on the sum of the transmit covariance matrices  $\sum_{j_b} \mathbf{G}_b^{RFH} \mathbf{V}_{j_b}^H \mathbf{P}_{j_b} \mathbf{V}_{j_b} \mathbf{G}_b^{RF}$ , once all the power matrices  $\mathbf{P}_{j_b}$  are updated in parallel. Solving (44) in parallel  $\forall j_b$  leads to the following optimal power allocation scheme

$$\mathbf{P}_{j_b} = (w_{j_b} (\mathbf{V}_{j_b}^H \mathbf{G}_b^H \mathbf{Z}_{j_b}^1 \mathbf{G}_b \mathbf{V}_{j_b})^{-1} - (\mathbf{V}_{j_b}^H \mathbf{G}_b^H \mathbf{Z}_{j_b}^2 \mathbf{G}_b \mathbf{V}_{j_b})^{-1})^+. \quad (45)$$

As a final step, the multiplier  $\psi_b$  can be searched with the Bisection method, similar to (36), and while doing so, the optimal power allocation for the DL user in the set  $\mathcal{D}_b$  can be computed in parallel according to (45).

Being a cooperative approach, after each synchronized iteration, each FD BS must exchange information about the updated digital beamformers, analog beamformer and combiner such that the neighbouring BSs could update their local variables in a synchronized manner. Continuous sharing of the information makes each FD BS aware of the generated interference at each iteration and hence enables correct adaption of the beamformers. Based on the per-link decomposition proposed above, the complete procedure to execute the cooperative P&D-HYBF for WSR maximization in a multi-cell mmWave FD system is formally stated in Algorithm 2.

*Remark 1:* We remark that C-HYBF would require complete CSI to the central node every CCT to optimize the beamformers. The presented P&D-HYBF requires that each FD BS is only aware of the local CSI, i.e., the interfering links appearing in the gradients, which results in significant reduction in the communication overhead. Moreover, as the computations are fully distributed in parallel on different base stations, it requires very small execution time.

*Remark 2:* A feedback from the neighbouring FD BSs is required only to update the out-cell local variables  $\overline{\mathbf{L}}_{j_b}^{Out}, \forall j_b$  and  $\overline{\mathbf{L}}_{k_b}^{Out}, \forall k_b$ . To further reduce the overhead, if the interference and CI channels among different cells vary slowly, the FD BSs can consider updating them only when these channels have changed significantly compared to the last feedback stage.

### C. On the Convergence of P&D-HYBF

The convergence proof for P&D-HYBF follows similarly from the proof stated for the C-HYBF scheme. Compared to C-HYBF scheme, the local variables have a different type of information saved for each communication link which dictate the gradients. Computing the beamformers given the information shared from the neighbouring BSs as the dominant generalized eigenvectors increase the WSR at each iteration for each link. However, the increase is

---

**Algorithm 2** Parallel and Distributed Hybrid Beamforming
 

---

**Given:** The rate weights, CSI and multiple processors in UL and DL  $\forall b$ .

**Initialize:**  $\mathbf{G}_b, \mathbf{V}_{j_b}, \mathbf{U}_{k_b}, \forall j_b \in \mathcal{D}_b, \forall k_b \in \mathcal{U}_b$  in each cell.

**Repeat until convergence**

$\forall b \in \mathcal{B}$ , share  $\mathbf{G}_b^{RF}, \mathbf{F}_b^{RF}$  and  $\mathbf{U}_{k_b}, \mathbf{V}_{j_b}, \forall k_b, \forall j_b$  with the neighbouring FD BSs.

**In parallel**  $\forall b$  ( $\forall k_b \in \mathcal{U}_b, \forall j_b \in \mathcal{D}_b$ .)

Update  $\overline{\mathbf{L}}_{j_b}^{In}, \overline{\mathbf{L}}_{k_b}^{In}$  from the memory and update  $\overline{\mathbf{L}}_{j_b}^{Out}$  and  $\overline{\mathbf{L}}_{k_b}^{Out}$  based on the feedback.

Update  $\overline{\mathbf{R}}_{k_b}^{-1}$  and  $\overline{\mathbf{R}}_{j_b}^{-1}$  from the memory.

**Solve in parallel**  $\forall b \in \mathcal{B}$

**Parallel DL for FD BS  $b$**

**Set:**  $\underline{\psi}_b = 0, \overline{\psi}_b = \psi_b^{max}$ .

Compute  $\overline{\mathbf{V}}_{j_b}$  in parallel with (41) and normalize it

Update  $\overline{\mathbf{R}}_{j_b}^{-1}$  and  $\overline{\mathbf{L}}_{j_b}^{In}$ ,  $\forall j_b$  from the memory

Compute  $\mathbf{G}_b^{RF}$  with (43), do unvec and get  $\angle \mathbf{G}_b^{RF}$

**Repeat until convergence**

set  $\psi_b = (\underline{\psi}_b + \overline{\psi}_b)/2$

**In parallel**  $\forall j_b$

Compute  $\mathbf{P}_{j_b}$  with (45), do SVD and set  $\mathbf{P}_{j_b} = \mathbf{D}_{P_{j_b}}$

Set  $\mathbf{Q}_{j_b} = \mathbf{G}_b \mathbf{V}_{j_b} \mathbf{P}_{j_b} \mathbf{V}_{j_b}^H \mathbf{G}_b^H$

**if** constraint for  $\psi_b$  is violated

set  $\underline{\psi}_b = \psi_b$ ,

**else**  $\overline{\psi}_b = \psi_b$

**Parallel UL for FD BS  $b$**

**Set:**  $\underline{\lambda}_{k_b} = 0, \overline{\lambda}_{k_b} = \lambda_{k_b}^{max}, \forall k_b$ .

Compute  $\overline{\mathbf{U}}_{k_b}^d$  (34) in parallel and normalize it

**Repeat until convergence in parallel**  $\forall k_b$

set  $\lambda_{k_b} = (\underline{\lambda}_{k_b} + \overline{\lambda}_{k_b})/2$

Compute  $\mathbf{P}_{k_b}$  in parallel with (35), do SVD and set  $\mathbf{P}_{k_b} = \mathbf{D}_{P_{k_b}}$

Set  $\mathbf{T}_b = \mathbf{U}_{k_b} \mathbf{P}_{k_b} \mathbf{U}_{k_b}^H$

**if** constraint for  $\lambda_{k_b}$  is violated

set  $\underline{\lambda}_{k_b} = \lambda_{k_b}$

**else**  $\overline{\lambda}_{k_b} = \lambda_{k_b}$

Update  $\overline{\mathbf{R}}_{k_b}^a, \overline{\mathbf{R}}_{k_b}^a, \forall k_b$ .

Compute  $\mathbf{F}_b^{RF}$  with (39) and get  $\angle \mathbf{F}_b^{RF}$ .

**Repeat**

**Quantize**  $\mathbf{G}_b^{RF}$  and  $\mathbf{F}_b^{RF}$ , with  $\mathcal{Q}_b(\cdot), \forall b$ .

---

different compared to C-HYBF as the local variables' information differs, thus resulting for the P&D-HYBF to converge to a different local optimum.

#### D. Computational Complexity Analysis

In this section, we present the per-iteration computational complexity for the C-HYBF and P&D-HYBF schemes. For such purpose, equal number of users in DL and UL in each cell, i.e.,

TABLE II: Per-iteration complexity for the C-HYBF and P&amp;D-HYBF.

$C_C$	$O(B^2U^2N_b^{RF^3} + B^2UDN_{j_b}^3 + B^2D^2N_{j_b}^3 + B^2DUN_b^{RF^3} + BM_b^{RF^2}M_b^2 + BN_b^{RF}N_b^2 + BDd_{j_b}M_b^{RF^2} + BDd_{k_b}N_{k_b}^2)$
$C_{P\&D}^{DL}, Z_{DL} = D$	$O(BDN_{j_b}^3 + BUN_b^{RF^3} + d_{j_b}M_b^{RF^2} + M_b^{RF^2}M_b^2)$
$C_{P\&D}^{DL}, Z_{DL} < D$	$O(KBDN_{j_b}^3 + KBUN_b^{RF^3} + Kd_{j_b}M_b^{RF^2} + M_b^{RF^2}M_b^2)$
$C_{P\&D}^{UL}, Z_{UL} = U$	$O(BUN_b^{RF^3} + BDN_{j_b}^3 + d_{k_b}N_{k_b}^2 + N_b^{RF}N_b^2)$
$C_{P\&D}^{UL}, Z_{UL} < U$	$O(NBUN_b^{RF^3} + NBDN_{j_b}^3 + Nd_{k_b}N_{k_b}^2 + N_b^{RF}N_b^2)$

$D_b = D$  and  $U_b = U$ ,  $\forall b \in \mathcal{B}$ , is assumed. Moreover, the number of antennas in each cell for the FD BSs, UL and DL users is also assumed to be the same.

Let us consider only the computational complexity of C-HYBF denoted with  $C_C$ , by ignoring its huge communication overhead to transfer complete CSI every CCT. Its one iteration consists in updating  $BD$  and  $BU$  digital beamformers for the DL and UL users, respectively, and  $B$  analog beamformers and  $B$  analog combiners by the central node. For P&D-HYBF, different computational processors have different computational burden and therefore we consider comparing its worst-case complexity. Namely, let  $Z_{DL}$  and  $Z_{UL}$  denote the number of processors dedicated for DL and UL by each FD BS, respectively. We consider the following two cases: 1)  $Z_{DL} = D$ ,  $Z_{UL} = U$ , and 2)  $Z_{DL} < D$ ,  $Z_{UL} < U, \forall b$ . The first case considers fully parallel implementation with the number of processors equal to the number of users. For such a case, the worst-case complexity in UL and DL is given for the processors which makes one update of the digital beamformer in UL and the analog combiner, and one update of the digital beamformer in DL and the analog beamformer, respectively, in each cell. The second case considers that the number of processors dedicated is less than the number of users. In such a case, each processor may have to update  $K$  and  $N$  digital beamformers in DL and UL, before updating the analog part. In such a case, the worst-case complexity in DL and UL is given for the processors which update  $K$  digital beamformers and the analog combiner, and  $N$  digital beamformers and the analog beamformer, respectively, in each cell. Considering the aforementioned details, the complexity analysis for the proposed schemes is provided in Table II, which clearly shows that P&D-HYBF requires significantly less computational power compared to the C-HYBF, and therefore very low-cost processors can be deployed at each FD BS.

## VI. SIMULATION RESULTS

This section presents simulation results to evaluate the performance of the proposed C-HYBF and P&D-HYBF schemes. For comparison, we consider the following benchmark schemes:

- A centralized *Fully Digital FD* scheme with the LDR noise.
- A centralized *Fully Digital HD* scheme with LDR noise, serving the UL and DL users by separating the resources in times. It is neither affected by the SI nor by the CI.

To compare the performance with a fully digital HD system, we define the additional gain in terms of percentage for an FD system over an HD system as

$$Gain = \frac{WSR_{FD} - WSR_{HD}}{WSR_{HD}} \times 100[\%], \quad (46)$$

where  $WSR_{FD}$  and  $WSR_{HD}$  are the network WSR for the FD and HD system, respectively. We assume the same SNR level for all the FD BSs, defined as  $SNR = p_b/\sigma_b^2$ , with transmit power  $p_b$  and thermal noise variance  $\sigma_b^2$ . We assume that the UL users and FD BSs transmit the same amount of power, i.e.,  $p_{k_b} = p_b, \forall k_b$ . The thermal noise level for DL users is set as  $\sigma_{j_b}^2 = \sigma_b^2, \forall j_b$ . The total transmit power is normalized to 1, and we choose the thermal noise variance to meet the desired SNR. We simulate a multi-cell network of  $B = 2$  cells, with each FD BS serving one DL and one UL user. P&D-HYBF is evaluated on a computer consisting of 4 computational processors, equal to the number of users in the network, i.e., fully parallel implementation, by using the parfor function in MATLAB. The FD BSs are assumed to have  $M_b = 100$  transmit and  $N_b = 60$  receive antennas, and the number of RF chains in transmission and reception is chosen as  $M_b^{RF} = N_b^{RF} = 32, 16, 10$  or  $8$ . The phase-shifters are assumed to be quantized with a uniform quantizer  $\mathbb{Q}_b(\cdot)$  of 10 or 4 bits. The DL and UL users are assumed to have  $N_{j_b} = N_{k_b} = 5$  antennas and are served with  $d_{j_b} = d_{k_b} = 2$  data streams. The number of paths for each device is chosen to be  $N_{k_b}^P = 3$ , and the AOA  $\theta_{k_b}^n$  and AOD  $\phi_{k_b}^n$  are assumed to be uniformly distributed in the interval  $\mathcal{U} \sim [-30^\circ, 30^\circ], \forall j_b, k_b$ . We assume uniform-linear arrays (ULAs) for the FD BSs and users. For the FD BSs, the transmit and the receive array are assumed to be separated with distance  $D_b = 20$  cm with a relative angle  $\Theta_b = 90^\circ$  and  $r_{m,n}$  in (5) is set given  $D_b$  and  $\Theta_b$  as in (9) [9]. The Rician factor is chosen to be  $\kappa_b = 1$  and the rate weights are set to be  $w_{k_b} = w_{j_b} = 1$ . Digital beamformers are initialized as the dominant eigenvectors of the channel covariance matrices of each user. The analog beamformers and combiners are initialized as the dominant eigenvectors of the sum of the channel covariance matrices across all the DL and UL users, respectively. The results reported herein are averaged over 100 channel realizations.

Fig. 5 shows the typical convergence behaviour of the proposed schemes compared to the fully digital FD system. It is evident that the proposed schemes experience a different increase



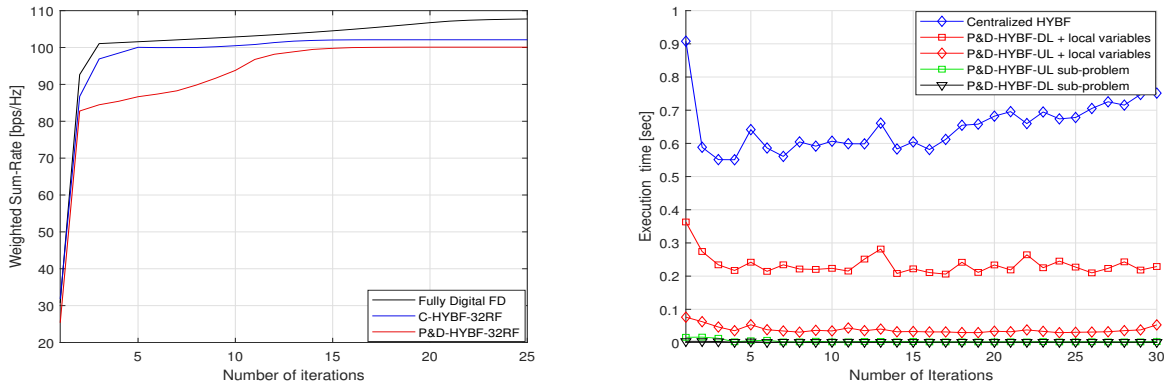


Fig. 5: Typical convergence behaviour of the proposed schemes. Fig. 6: Execution time for the C-HYBF and the P&D HYBF schemes with 32-RF chains.

in the WSR at each iteration and converge to different local optimum points, but the difference in the achieved WSR is negligible. We also remark that as the P&D-HYBF converges in a few iterations, a minimal amount of communication overhead to share information about the updated variables is required. Fig. 6 shows the typical execution time to run the C-HYBF and the P&D-HYBF with 32 RF chains. We can see that the former requires significant computational time as it can only update different variables iteratively based on alternating optimization, one after the other. Transferring full CSI to the central node and communicating back the optimized variables to all cells will add significant additional time, which is ignored in the simulations. For the latter, computation of the local variables takes place in parallel at each FD BS which has to compute only the variables associated with its users based on the feedback on multiple processors. It is evident that the P&D-HYBF requires  $\sim 1/21$  and  $\sim 1/2.3$  less time in UL and DL, respectively than the average execution time of C-HYBF. The complexity of P&D-HYBF in DL is dominated by the computation of one large generalized dominant eigenvector to update the vectorized analog beamformer, which has complexity  $O(M_b^{RF^2} M_b^2)$ . In UL, complexity is dominated by the computation of the analog combiner, which is only  $O(N_b^{RF} N_b^2)$ . The execution time to solve one sub-problem for the bottom layers in UL and DL is also shown, which is negligible compared to the average execution time of C-HYBF. From the complexity analysis reported in Table II, we can expect the execution time of C-HYBF to scale quadratically as the number of users or cells increases. On the other hand, P&D-HYBF requires significantly less execution time and is expected to increase only linearly as the network grows.

Fig. 7 shows the average WSR achieved with both schemes as a function of the LDR noise

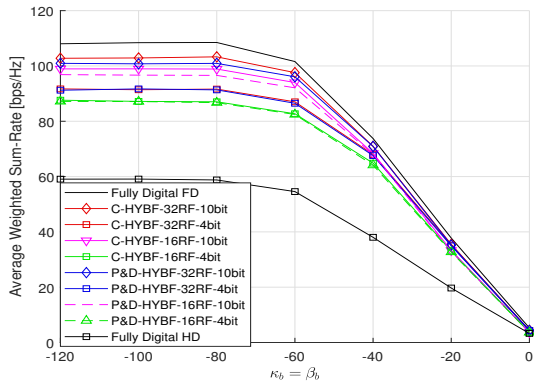


Fig. 7: Average WSR as a function of the LDR noise with SNR= 20 dB.

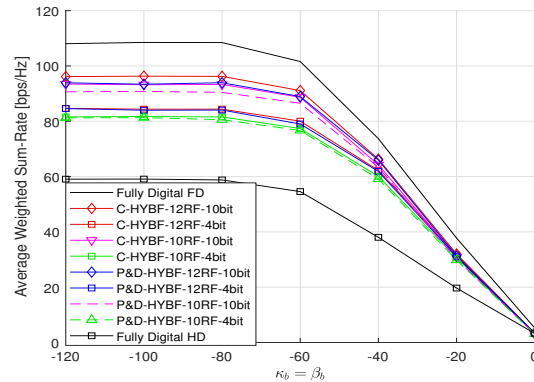


Fig. 8: Average WSR as a function of the LDR noise with SNR= 20 dB.

with 32 or 16 RF chains and 10 or 4 bits phase-resolution. It is visible that the P&D-HYBF performs very close to the C-HYBF scheme with the same number of RF chains and phase resolution. Fully digital FD achieves  $\sim 83\%$  of additional gain than the fully digital HD for any LDR noise level. For a low LDR noise level  $k_b < -80$  dB, C-HYBF and P&D-HYBF with 32 RF chains achieve  $\sim 74, 55$  and  $\sim 71, 54\%$  additional gain and with 16 RF chains they achieve  $\sim 67\%, 48\%$  and  $\sim 64\%, 47\%$  additional gain with 10, 4 bits phase-resolution, respectively. We can also see that when the LDR noise variance increases, the achievable WSR for both the FD and HD systems decreases considerably. Fig. 8 shows the average WSR as function of the LDR noise with only 12 or 10 RF chains and with 10 or 4 bits phase-resolution. For LDR noise  $k_b \leq 80$  dB, C-HYBF and P&D-HYBF with 12 RF chains achieves  $\sim 60, 43\%$  and  $\sim 57, 43\%$  additional gain and with 10 RF chains they achieve additional gain of  $\sim 58, 38\%$  and  $\sim 53, 37\%$  with 10, 4 bit phase-resolution, respectively. Fig. 7-8 exhibits the detrimental effect of the LDR noise on the maximum achievable WSR with HYBF for both the schemes for mmWave FD and motivates to deploy RF circuitry, which generates small LDR noise. It is to be noted that P&D-HYBF achieves similar performance as the C-HYBF scheme at any LDR noise level.

Fig. 9 shows the average WSR as a function of the SNR with 32 and 16 RF chains and with 10 or 4 bit phase-resolution affected with LDR noise  $k_b = -80$  dB, in comparison with the benchmark schemes. We can see that a fully digital FD system achieves  $\sim 94\%$  and  $\sim 82\%$  additional gain at low and high SNR, respectively. With 32 RF chains and 10 bit phase-resolution, the C-HYBF scheme achieves  $\sim 79\%$  gain at all the SNR levels and the P&D-HYBF achieves  $\sim 77\%$  and  $\sim 68\%$  gain at low and high SNR, respectively. As the phase-resolution decreases to 4-bits, we can see that the loss in WSR compared to the 10-bit phase-resolution case is

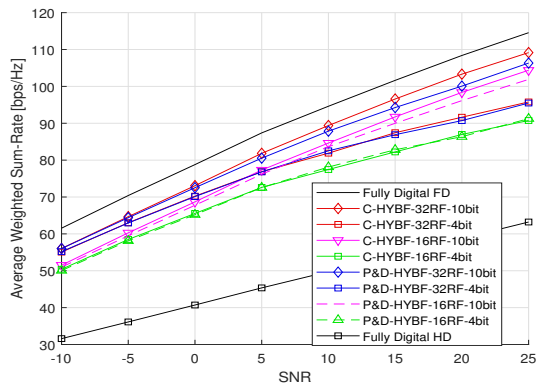


Fig. 9: Average WSR as a function of the SNR with LDR noise  $\kappa_{k_b} = -80$  dB.

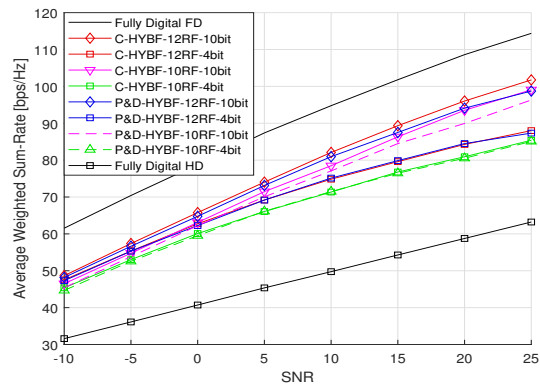


Fig. 10: Average WSR as a function of the SNR with LDR noise  $\kappa_{k_b} = -80$  dB.

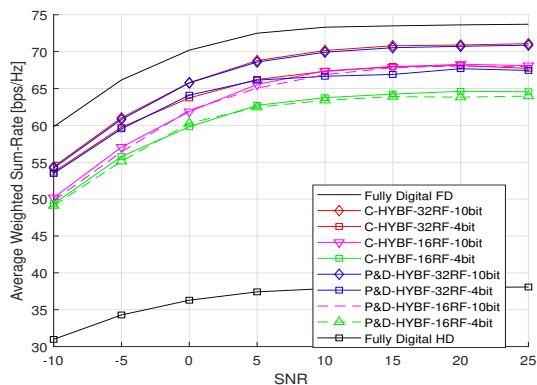


Fig. 11: Average WSR as function of the SNR with LDR noise  $\kappa_{k_b} = -40$  dB.

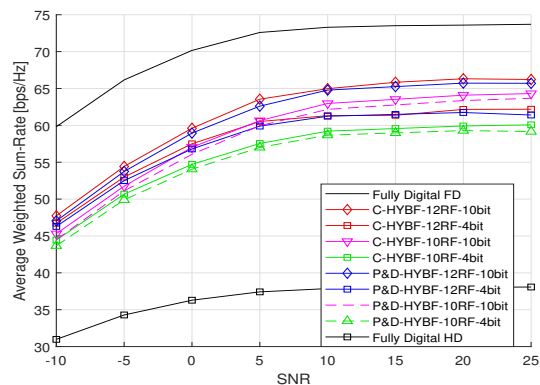


Fig. 12: Average WSR as a function of the SNR with LDR noise  $\kappa_{k_b} = -40$  dB.

much more evident at high SNR. Still, with 16 RF chains and 10 or 4 bit phase-resolution, both schemes significantly outperform the fully digital HD scheme for any SNR level. Fig. 10 shows the average WSR as a function of the SNR with same LDR noise level as in Fig. 9, i.e.,  $k_b = -80$  dB, but with 10 or 12 RF chains and 10 or 4 bit phase-resolution. The achieved average WSR presents a similar behaviour as in the case of a high number of RF chains, and it is visible that the proposed schemes significantly outperform the fully digital HD system also with very low number of RF chains and phase-resolution. Moreover, P&D-HYBF achieves similar performance as the C-HYBF scheme regardless of the phase resolution and number of RF chains.

Fig. 11 shows the achieved average WSR as a function of the SNR with LDR noise  $k_b = -40$  dB, which reflects highly non-ideal RF circuitry. We can see that when the LDR noise dominates, reduction of the thermal noise variance has negligible effect on the effective signal-to-LDR-plus-thermal-noise ratio (SLNR). Therefore, dominance of the LDR noise variance acts

as a ceiling to the effective SLNR ratio which limits the achievable WSR, tending to saturate at SNR= 10 dB. We can also see that with a large LDR noise level, C-HYBF and P&D-HYBF still perform similarly with the same phase-resolution and RF chains. At high SNR, both schemes achieve higher WSR with 16 RF chains and 10 bit phase-resolution than the case of 32 RF chains and 4 bit phase-resolution. Fig. 12 shows the average WSR as a function of the SNR with only 10 or 12 RF chains and with 10 or 4 bit phase-resolution, clearly showing that the proposed schemes can still significantly outperform the full digital HD system. Fig. 12 also shows that both schemes with 10 RF chains and 10 bit phase resolution are more robust to the LDR noise than the case of 12 RF chains and 4 bit phase-resolution, thus motivating to deploy high resolution phase-shifters at the analog stage rather than deploying more number of RF chains, which not only requires higher cost but also it will not yield higher gains than the high resolution phase shifters case.

From the results presented above, we can conclude that both the proposed HYBF schemes achieve significant additional gain and outperform the fully digital HD system with only a few RF chains and low phase resolution. Furthermore, both the designs achieve similar performance, but P&D-HYBF is much more attractive as it eliminates the problem of transferring full CSI to the central node at every channel CCT, thus reducing the communication overhead significantly. The per-link independent decomposition enables each FD BS to solve its local sub-problems independently on multiple computational processors, and it results to be also highly scalable as its complexity increases only linearly as a function of the number of users and FD BSs. On the other hand, besides the massive communication overhead, C-HYBF has a quadratic dependency on the computational complexity and requires massive computational power per-iteration to update all the variables jointly based on alternating optimization. P&D-HYBF imposes a minimal computational burden on each processor due to per-link independent decomposition and as the computations are made in parallel, it requires considerably less execution time. By investigating the execution time, we learned that the P&D-HYBF requires  $\sim 1/21$  and  $\sim 1/2.3$  less execution time in UL and DL, respectively, compared to the C-HYBF scheme. Such time is expected to increase only linearly with the network size and density for P&D-HYBF, meanwhile for C-HYBF it will scale quadratically. Finally, as the P&D-HYBF converges in a few iterations, a very small amount of information exchange is required among the FD BSs.

## VII. CONCLUSION

This article presented two HYBF schemes for WSR maximization in multi-cell mmWave mMIMO FD systems. Firstly, a C-HYBF scheme based on alternating optimization is presented. However, C-HYBF requires massive communication overhead to exchange information between the FD network and the central node. Moreover, very high computational power is required to optimize numerous variables jointly. To overcome these drawbacks, a very low-complexity P&D-HYBF design is proposed, which enables each FD BS to solve its local per-link independent sub-problems simultaneously on different computational processors, which drastically reduces the communication overhead. Its complexity scales only linearly as a function of the network size, making it highly scalable and enabling the deployment of low-cost computational processors. Simulation results show that the proposed HYBF designs achieve similar average WSR and significantly outperform the centralized fully digital HD systems with only a few RF chains.

## REFERENCES

- [1] C. K. Sheemar, “Hybrid beamforming techniques for massive mimo full duplex radio systems,” Ph.D. dissertation, EURECOM, 2022.
- [2] X. Wang, L. Kong, F. Kong, F. Qiu, M. Xia, S. Arnon, and G. Chen, “Millimeter wave communication: A comprehensive survey,” *IEEE Communications Surveys & Tutorials*, vol. 20, no. 3, pp. 1616–1653, 2018.
- [3] S. Rangan, T. S. Rappaport, and E. Erkip, “Millimeter-wave cellular wireless networks: Potentials and challenges,” *Proceedings of the IEEE*, vol. 102, no. 3, pp. 366–385, Feb. 2014.
- [4] A. F. Molisch, V. V. Ratnam, S. Han, Z. Li, S. L. H. Nguyen, L. Li, and K. Haneda, “Hybrid beamforming for massive mimo: A survey,” *IEEE Communications magazine*, vol. 55, no. 9, pp. 134–141, 2017.
- [5] I. P. Roberts, J. G. Andrews, H. B. Jain, and S. Vishwanath, “Millimeter-wave full duplex radios: New challenges and techniques,” *IEEE Wirel. Commun.*, vol. 28, no. 1, pp. 36–43, Feb. 2021.
- [6] C. B. Barneto, S. D. Liyanaarachchi, M. Heino, T. Riihonen, and M. Valkama, “Full duplex radio/radar technology: The enabler for advanced joint communication and sensing,” *IEEE Wireless Commun.*, vol. 28, no. 1, pp. 82–88, Feb. 2021.
- [7] H. Alves, T. Riihonen, and H. A. Suraweera, *Full-Duplex Communications for Future Wireless Networks*. Springer, 2020.
- [8] M. T. Kabir and C. Masouros, “A scalable energy vs. latency trade-off in full-duplex mobile edge computing systems,” *IEEE Trans. Commun.*, vol. 67, no. 8, pp. 5848–5861, May 2019.
- [9] K. Satyanarayana, M. El-Hajjar, P.-H. Kuo, A. Mourad, and L. Hanzo, “Hybrid beamforming design for full-duplex millimeter wave communication,” *IEEE Trans. Veh. Technol.*, vol. 68, no. 2, pp. 1394–1404, Feb. 2018.
- [10] J. Palacios, J. Rodriguez-Fernandez, and N. González-Prelcic, “Hybrid precoding and combining for full-duplex millimeter wave communication,” in *IEEE Global Commun. Conf. (GLOBECOM)*, Dec. 2019, pp. 1–6.
- [11] R. López-Valcarce and N. González-Prelcic, “Analog beamforming for full-duplex millimeter wave communication,” in *IEEE 16th Int. Symp. Wirel. Commun. Syst. (ISWCS)*, Aug. 2019, pp. 687–691.
- [12] C. K. Sheemar and D. Slock, “Hybrid beamforming and combining for millimeter wave full duplex massive MIMO interference channel,” *arXiv preprint arXiv:2108.00465*, 2021.

- [13] Y. Cai, K. Xu, A. Liu, M. Zhao, B. Champagne, and L. Hanzo, “Two-timescale hybrid analog-digital beamforming for mmwave full-duplex MIMO multiple-relay aided systems,” *IEEE J. Sel. Areas Commun.*, vol. 38, no. 9, pp. 2086–2103, Jun. 2020.
- [14] Z. Luo, L. Zhao, L. Tonghui, H. Liu, and R. Zhang, “Robust hybrid precoding/combining designs for full-duplex millimeter wave relay systems,” *IEEE Trans. Veh. Technol.*, vol. 70, no. 9, pp. 9577–9582, Jul. 2021.
- [15] C. K. Sheemar and D. Slock, “Massive MIMO mmwave full duplex relay for IAB with limited dynamic range,” in *IEEE 11th IFIP Int. Conf. on New Techn., Mob. and Sec. (NTMS)*, Apr. 2021, pp. 1–5.
- [16] R. López-Valcarce and N. González-Prelcic, “Beamformer design for full-duplex amplify-and-forward millimeter wave relays,” in *IEEE 16th Int. Symp. Wirel. Commun. Syst. (ISWCS)*, Oct. 2019, pp. 86–90.
- [17] J. M. B. da Silva, A. Sabharwal, G. Fodor, and C. Fischione, “1-bit phase shifters for large-antenna full-duplex mmwave communications,” *IEEE Trans. Wirel. Commun.*, vol. 19, no. 10, pp. 6916–6931, Jul. 2020.
- [18] I. P. Roberts, H. B. Jain, and S. Vishwanath, “Equipping millimeter-wave full-duplex with analog self-interference cancellation,” in *IEEE Int. Conf. Commun. Work. (ICC Workshops)*, Jun. 2020, pp. 1–6.
- [19] I. P. Roberts, J. G. Andrews, and S. Vishwanath, “Hybrid beamforming for millimeter wave full-duplex under limited receive dynamic range,” *arXiv preprint arXiv:2012.11647*, 2020.
- [20] C. K. Sheemar, C. K. Thomas, and D. Slock, “Practical hybrid beamforming for millimeter wave massive mimo full duplex with limited dynamic range,” *IEEE Open Journal of the Communications Society*, vol. 3, pp. 127–143, 2022.
- [21] M. A. Islam, G. C. Alexandropoulos, and B. Smida, “Integrated sensing and communication with millimeter wave full duplex hybrid beamforming,” *arXiv preprint arXiv:2201.05240*, 2022.
- [22] J.-H. Lee and O.-S. Shin, “Full-duplex relay based on distributed beamforming in multiuser mimo systems,” *IEEE transactions on vehicular technology*, vol. 62, no. 4, pp. 1855–1860, 2012.
- [23] X. Xu, X. Chen, M. Zhao, S. Zhou, C.-Y. Chi, and J. Wang, “Power-efficient distributed beamforming for full-duplex mimo relaying networks,” *IEEE Transactions on Vehicular Technology*, vol. 66, no. 2, pp. 1087–1103, 2016.
- [24] J.-H. Lee and O.-S. Shin, “Distributed beamforming approach to full-duplex relay in multiuser mimo transmission,” in *2012 IEEE Wireless Communications and Networking Conference Workshops (WCNCW)*. IEEE, 2012, pp. 278–282.
- [25] T. M. Kim, H. J. Yang, and A. J. Paulraj, “Distributed sum-rate optimization for full-duplex MIMO system under limited dynamic range,” *IEEE Signal Process. Lett.*, vol. 20, no. 6, pp. 555–558, Feb. 2013.
- [26] G. Scutari, F. Facchinei, and L. Lampariello, “Parallel and distributed methods for constrained nonconvex optimization—part i: Theory,” *IEEE Trans. Signal*, vol. 65, no. 8, pp. 1929–1944, Dec. 2016.
- [27] G. Scutari, F. Facchinei, P. Song, D. P. Palomar, and J.-S. Pang, “Decomposition by partial linearization: Parallel optimization of multi-agent systems,” *IEEE Trans. Signal*, vol. 62, no. 3, pp. 641–656, Nov. 2013.
- [28] B. P. Day, A. R. Margetts, D. W. Bliss, and P. Schniter, “Full-duplex bidirectional MIMO: Achievable rates under limited dynamic range,” *IEEE Trans. Signal Process.*, vol. 60, no. 7, pp. 3702–3713, Apr. 2012.
- [29] I. P. Roberts, J. G. Andrews, and S. Vishwanath, “Hybrid beamforming for millimeter wave full-duplex under limited receive dynamic range,” *IEEE Transactions on Wireless Communications*, 2021.
- [30] P. Stoica and Y. Selen, “Cyclic minimizers, majorization techniques, and the expectation-maximization algorithm: A refresher,” *IEEE Signal Process. Mag.*, vol. 21, no. 1, pp. 112–114, Feb. 2004.
- [31] S. Boyd, S. P. Boyd, and L. Vandenberghe, *Convex Optimization*. Cambridge university press, 2004.